

INFORMATION TO USERS

This material was produced from a microfilm copy of the original document. While the most advanced technological means to photograph and reproduce this document have been used, the quality is heavily dependent upon the quality of the original submitted.

The following explanation of techniques is provided to help you understand markings or patterns which may appear on this reproduction.

1. The sign or "target" for pages apparently lacking from the document photographed is "Missing Page(s)". If it was possible to obtain the missing page(s) or section, they are spliced into the film along with adjacent pages. This may have necessitated cutting thru an image and duplicating adjacent pages to insure you complete continuity.
2. When an image on the film is obliterated with a large round black mark, it is an indication that the photographer suspected that the copy may have moved during exposure and thus cause a blurred image. You will find a good image of the page in the adjacent frame.
3. When a map, drawing or chart, etc., was part of the material being photographed the photographer followed a definite method in "sectioning" the material. It is customary to begin photoing at the upper left hand corner of a large sheet and to continue photoing from left to right in equal sections with a small overlap. If necessary, sectioning is continued again — beginning below the first row and continuing on until complete.
4. The majority of users indicate that the textual content is of greatest value, however, a somewhat higher quality reproduction could be made from "photographs" if essential to the understanding of the dissertation. Silver prints of "photographs" may be ordered at additional charge by writing the Order Department, giving the catalog number, title, author and specific pages you wish reproduced.
5. PLEASE NOTE: Some pages may have indistinct print. Filmed as received.

Xerox University Microfilms

300 North Zeeb Road
Ann Arbor, Michigan 48106

77-2366

CHANG, Lu-hsi, 1939-
LIGHT AND ELECTRON MICROSCOPIC STUDIES
OF THE POSTEMBRYONIC STAGES OF THE
TAPEWORM, HYMNOLEPIS DIMINUTA
(CYCLOPHYLLIDEA, HYMNOLEPIDIDAE).

The Ohio State University, Ph.D., 1976
Zoology

Xerox University Microfilms, Ann Arbor, Michigan 48106

LIGHT AND ELECTRON MICROSCOPIC STUDIES OF THE POSTEMBRYONIC
STAGES OF THE TAPEWORM, HYMENOLEPIS DIMINUTA
(CYCLOPHYLLIDEA, HYMENOLEPIDIDAE)

DISSERTATION

Presented in Partial Fulfillment of the
Requirements for the Degree Doctor of
Philosophy in the Graduate School
of The Ohio State University

By

Lu-hsi Chang, B.S., M.S.

The Ohio State University

1976

Reading Committee:

John L. Crites

Willard C. Myser

Wayne B. Parrish

Advisor

Approved By

Wayne B. Parrish
Advisor

Department of Zoology

ACKNOWLEDGMENTS

I am grateful to my adviser Dr. Wayne B. Parrish for the provision of research facilities and his helpful advice and to Dr. John L. Crites for the inspiration of this research during the course of this study. I wish to thank Dr. Willard C. Myser and Dr. Frank F. Jaszcs, Jr. for their critically reviewing of the manuscript.

The tapeworms, Hymenolepis diminuta, were obtained through the kindness of Dr. Peter W. Pappas. Thanks are due also to Mr. John M. McCabe for supplying grain beetles, Tenebrio molitor.

VITA

- July 12, 1939 Born - Shantung, China
- 1968 B.Sc., National Taiwan Normal University,
Taiwan, China
- 1968-1970 Teaching Assistance, Department of
Biology, National Taiwan Normal Uni-
versity, Taiwan, China
- 1972 M.S., The Ohio State University,
Columbus, Ohio
- 1971-1976 Teaching Associate, Department of
Zoology, The Ohio State University,
Columbus, Ohio

FIELDS OF STUDY

Major Field: Parasitology

Studies in Parasitology. Professor John L Crites

Studies in Electron Microscopy. Professor Wayne B. Parrish

Studies in Histology. Professor Thomas G. Hayes and Adelph G.
Ackerman

Studies in Developmental Biology. Professor Roy A. Tassava

TABLE OF CONTENTS

	Page
ACKNOWLEDGMENTS	ii
VITA	iii
LIST OF FIGURES	v
INTRODUCTION	1
MATERIALS AND METHODS	5
RESULTS	7
I. Light Microscopy	
II. Electron Microscopy	
DISCUSSION	31
SUMMARY	44
APPENDIX I	46
Figures	
APPENDIX II	163
Preparation of a polychrome stain	
LITERATURE CITED	164

LIST OF FIGURES

Figure	Page
1. Light photomicrograph (LPM) of a stage two larva	46
2. LPM of a high-power view of the anterior end of a stage two larva	46
3. LPM of a stage two larva showing the distribution of cell types one, two, and three	48
4. LPM of a high-power view of a type three cell	48
5. LPM of the forebody of a stage three larva.	50
6. LPM of a high-power view of the rudimentary sucker of a stage three larva	50
7. LPM of a high-power view of a type four cell of a rudimentary sucker.	52
8. LPM of the transitional zone of a stage three larva	52
9. LPM of a high-power view of the transitional zone of a stage three larva	54
10. LPM of a high-power view of the loose network in the middle of the transitional zone of a stage three larva	54
11. LPM of a high-power view of the transitional zone of a stage three larva	56
12. LPM of the midbody of a stage three larva	56
13. LPM of a high-power view of the subtegumentary cellular layer of the midbody of a stage three larva	58
14. LPM of a high-power view of the outer and inner fibrous layers of the midbody of a stage three larva.	58
15. LPM of the hindbody of a stage three larva.	60

Figure	Page
16. LPM of a high-power view of the subtegumentary cellular layer of the hindbody of a stage three larva	60
17. LPM of a high-power view of the core of the hindbody of a stage three larva.	62
18. LPM of the anterior end of a stage five larva	62
19. LPM of the middle portion of the anterior canal of a stage five larva	64
20. LPM of the end of anterior canal of a stage five larva.	64
21. LPM of the plug of a stage five larva	66
22. LPM of the invaginated scolex of a stage five larva	66
23. LPM of a high-power view of the invaginated scolex of a stage five larva	68
24. LPM of the anterior end of the invaginated scolex of a stage five larva	68
25. LPM of a high-power view of a stage five larval capsule	70
26. LPM of a high-power view of both loose and dense fibrous layers of a stage five larval capsule	70
27. LPM of the tail of a stage five larva	72
28. LPM of a high-power view of the tail of a stage five larva.	72
29. Electron photomicrograph (EPM) of a high-power view of a beetle haemocyte.	74
30. EPM of a layer of beetle haemocytes attached to a stage two larva	76
31. EPM of a high-power view of an active beetle haemocyte which is attached to a stage two larva.	78
32. EPM of a beetle haemocyte undergoes degradative changes	80

Figure	Page
33. EPM of a high-power view of a cytolyzed beetle haemocyte	82
34. EPM of a low-power view of a subtegumentary cell.	82
35. EPM of the tegument and subtegumentary cell of a stage two larva	84
36. EPM of a high-power view a muscle cell of a stage two larva	86
37. EPM of a high-power view of a cytoplasmic process of a muscle cell of a stage two larva	86
38. EPM of the subtegumentary cellular layer of a stage two larva	88
39. EPM of a high-power view of type one cells.	90
40. EPM of an oblique section of a larval hook.	92
41. EPM of a high-power view of the basal region of a larval hook.	92
42. EPM of a high-power view of a decomposed area of a larval hook muscle.	94
43. EPM of a high-power view of an oblique section of a larval hook.	96
44. EPM of the tegument and muscles of the forebody of a stage three larva.	98
45. EPM of the tegument of the forebody of a stage three larva	100
46. EPM of a high-power view of dense bodies among myofilaments.	100
47. EPM of a high-power view of the medullary region of the forebody of a stage three larva.	102
48. EPM of the medullary region of the forebody of a stage three larva	102
49. EPM of the transitional zone of a stage three larva	104
50. EPM of a high-power view of a terminal organ of a protonephridial system of a stage three larva	104

Figure	Page
51. EPM of a high-power view of an oblique section through a terminal organ of a stage three larva	106
52. EPM of a longitudinal section of a terminal organ of a stage three larva	106
53. EPM of a high-power view of a developing collecting duct cell of a stage three larva.	108
54. EPM of type four cells and their cytoplasmic processes	110
55. EPM of a high-power view of a type four cell and its cytoplasmic processes	112
56. EPM of cytoplasmic processes of type four cells are in contact with a muscle cell	114
57. EPM of a calcareous corpuscle formation cell is surrounded by cytoplasmic processes of type four cells.	116
58. EPM of a calcareous corpuscle formation cell.	118
59. EPM of a young calcareous corpuscle formation cell consists of less-dense matrix.	120
60. EPM of a high-power view of a muscle cell of a stage three larva	120
61. EPM of a high-power view of type five cells of a stage three larva	122
62. EPM of a low-power view of the midbody of a stage three larva	124
63. EPM of the outer fibrous layer of a stage three larva	126
64. EPM of a high-power view of a type four cell and its highly branched cytoplasmic processes	128
65. EPM of the tegument and its cell body of a stage five larva.	130
66. EPM of the tegument and subtegumentary cellular layer of a stage five larva	132

Figure	Page
67. EPM of the tegument and a vesiculated subtegumentary cell of a stage five larva	134
68. EPM of the tegument and type five cells of a stage five larva.	136
69. EPM of a low-power view of the loose fibrous layer of a stage five larva	138
70. EPM of a high-power view of a terminal organ of a protonephridial system of a stage five larva.	138
71. EPM of a high-power view of the interdigitated region of the terminal organ of a stage five larva	140
72. EPM of a high-power view of the tip of the flame of a stage five larva	140
73. EPM of a low-power view of the dense fibrous layer of a stage five larva	142
74. EPM of a high-power view of collecting ducts of a stage five larva.	142
75. EPM of the loose fibrous layer, the dense fibrous layer, and the invaginated scolex of a stage five larva.	144
76. EPM of a high-power view of the dense fibrous layer of a stage five larva	146
77. EPM of a low-power view of the dense fibrous layer of a stage five larva with several calcareous corpuscles.	148
78. EPM of a atrophing calcareous corpuscle formation cell of a stage five larva	150
79. EPM of the tegument of an invaginated scolex of a stage five larva.	152
80. EPM of a low-power view of the sucker region of the invaginated scolex of a stage five larva	154
81. EPM of a low-power view of the inter-sucker region of the invaginated scolex of a stage five larva	156

Figure	Page
82. EPM of a high-power view of the anterior canal of a stage five larva	158
83. EPM of a low-power view of the plug of a stage five larva.	160
84. A growth curve of the postembryonic development of <u>Hymenolepis diminuta</u> in the intermediate hosts	162

INTRODUCTION

The life history of the rat tapeworm Hymenolepis diminuta involves two hosts, a definitive host, the rat, and an intermediate host, the grain beetle. Monoecious adult worms produce eggs which contain oncospheres. Eggs containing oncospheres pass out of the definitive host and are eaten by beetles. The oncospheres are freed in the beetle midgut and penetrate through the intestinal wall by using their hooks and penetration glands. They attach to the outside of the intestinal wall and to the Malpighian tubules where they immediately undergo development and metamorphosis (Lethbridge, 1971). If beetles are kept at 30°C, mature infective cysticercoids will develop in the haemocoel within twelve days. If infected beetles with mature cysticercoids are eaten by the definitive host, the cysticercoids will develop to sexually-reproducing adults within fifteen days. The life history of the rat tapeworm can be completed within a month.

Rat tapeworm development consists of: (a) embryonic development which occurs in the adult tapeworm and results in oncospheres; (b) post-embryonic development which occurs in the beetle and results in cysticercoids; and (c) strobilization and sexual maturation which occur in the rat and result in adults. This manuscript is concerned with the postembryonic development of the rat tapeworm.

Postembryonic development of tapeworm with cysticercoid larval stage has been studied by several investigators. These studies have provided the foundation on which the present study is based. Therefore, in the following sections the literature of the postembryonic development is reviewed.

The postembryonic development of the rat tapeworm has been arbitrarily divided into five stages (stage 1 through stage 5) by Voge and Heyneman (1957) and by Rothman (1957). These investigators also established a time table for the postembryonic development in the intermediate host Tribolium confusum (the confused flour beetle) which were maintained at 30°C. Moreover, they studied the succession of gross morphological changes which occurred in the tapeworm larvae as they developed in the haemocoel of the beetle.

The first histological study of a fully developed cysticeroid of Hymenolepis diminuta was made by Voge (1960a) utilizing light microscopy. Ultrastructure of the capsule and incapsulated scolex of H. diminuta have been studied by Ubelaker et al (1970a), Allison et al (1972), and Cooper et al (1975). They described the different tissue layers, fibrous components, and cell types of the capsule, the tegument, basement membrane, muscle layers, and the medullary region of the incapsulated scolex. Eventually, the morphology and histology of fully developed cysticeroids of H. diminuta are fairly well-documented. Both Voge (1960a) and Ubelaker et al (1970a) suggested that additional study of the various stages in cysticeroid development would be essential in order to understand the histological structure of the fully developed cysticeroid and to confirm the roles of different cells during postembryonic development. Voge (1960b), on the basis of light microscopy, described the major histological changes occurring during the postembryonic development of Hymenolepis diminuta. She discussed the origin of several tissues and also the cell types involved in the formation of these tissues. Because of the complexity of

organization, the cellular density, and the small size of larval cells, she experienced difficulty in interpreting the observations. At this time, she pointed out that new methods of study, including electron microscopy, were needed to reveal the histogenesis in the cysticeroid.

The only ultrastructural study of larval stages of the cysticeroid was made by Collin (1970). He described the cell types of stage two and three larvae of H. citelli. However, he neither determined the fate of these cells nor did he study the relationship between cellular and tissue components.

These investigators neglected to study certain structures of the cysticeroid, such as the protonephridial system and the calcareous corpuscle. Protonephridial systems are found in a wide range of invertebrate groups, including the platyhelminthes. The morphology and the physiology of protonephridial systems in many other groups have been studied by several investigators (Wilson, 1974; Howells, 1969; Wilson, 1969; Bonsdorff and Telkka, 1966). Their morphology is well-established. However, there are no morphogenetic studies and their physiological role is still not completely understood. The ultrastructure and formation of calcareous corpuscles has been reported for several species of adult tapeworms (Nieland and Brand, 1969; Chowdhur et al, 1962; Brand et al, 1960). However, there is no information available of calcareous corpuscle formation in larval stages.

The purpose of this study is to describe tissues and their cellular components in larval stages two through five of Hymenolepis diminuta. The roles and fates of these cells will be examined. The cytomorphogenesis of teguments, muscles, calcareous corpuscles and the

protonephridial system will be described, stage by stage, with hope to establish the pattern of cysticeroid postembryonic development.

MATERIAL AND METHODS

Laboratory rats of various ages were experimentally infected with rat tapeworms, Hymenolepis diminuta. Grain beetles, Tenebrio monitor, which serve as intermediate hosts for this tapeworm, were obtained from the insect culture laboratory of the Entomology Department, The Ohio State University.

Infected rats were sacrificed, dissected and tapeworms were removed from the small intestine and placed in Ringer's "warm" solution. Gravid proglottids were cut off and embryonated eggs were recovered by mincing the proglottids on a piece of filter paper. Infections were accomplished by feeding minced gravid proglottids to beetles, previously starved for five to seven days. The feeding time varied from two to five hours. Infected beetles were kept at 25°C in small containers and maintained on a diet of "Milk Bone" dog biscuits. The beetles were dissected in Ringer's "cold" solution and examined under the dissecting microscope. Dissection and examination were carried out in an ice bath. Larvae (cysticercoïds) were teased free from the intestine and Malpighian tubules at five, seven, nine, thirteen and twenty-three day intervals following experimental infection. Approximately two-hundred infected beetles were examined in the course of this study.

The larvae were prepared for light microscopy and electron microscopy by fixing in 4% phosphate-buffered glutaraldehyde (pH 7.2) at 4°C for three hours. After fixation, the larvae were rinsed in a phosphate-buffered wash and postfixed in 1% phosphate-buffered osmium

tetroxide, at 4°C (Millonig, 1961). Following postfixation, the larvae were washed in 35% ethanol and stained in 2% aqueous uranyl acetate for thirty-five minutes. The larvae were then dehydrated in an increasing series of ethanol to 95%, five minutes for each concentration. Final dehydration was accomplished in two changes of 100% ethanol (5 minutes each). Spurr's low-viscosity epoxy resin (Spurr, 1969) was employed as the embedding medium. The following ratios (100% ethanol : 100% resin) and times used for infiltration were: 3 : 1, for twenty minutes; 1 : 1, for forty minutes; 1 : 3, for one hour. The larvae were then placed in full strength resin for fifteen hours. Finally, the larvae were embedded in fresh resin for twenty-four hours in an oven at 70°C.

Thick sections (0.5 μm . to 1 μm .) were cut on a Porter-Blum MT-2 ultramicrotome using glass knives. Thick sections were placed on glass slides and stained with a polychrome stain (Sato and Shamoto, 1973) for observations with the light microscope. Thin sections (pale gold to gray) were cut with either glass or diamond knives, floated on water, spread with chloroform, and picked up on two-hundred mesh copper grids. Thin sections were double-stained with saturated aqueous uranyl acetate (Watson, 1958) and lead citrate (Reynolds, 1963). Sections were examined with an RCA-3G electron microscope. Photomicrographs were made using DuPont Cromar Ortho-Litho Cos-7 film. A Simmon Omega D enlarger was used to make prints on Kodak F-4 photographic paper.

RESULTS

I. Light Microscopy

A. Stage Two Larvae:

Stage two larvae were obtained from beetles five to seven days after experimental infection. A stage two larva is spherical and contains a central cavity (Fig. 1). The tegument, the outermost layer of the larva, has a brush border of irregularly-arranged, fine, densely packed filaments. A layer of host cells, presumably beetle haemocytes, are always attached to the brush border. Cells are not evenly distributed over the peripheral area underneath the tegument. One area of the spherical structure has four or five layers of cells while the remaining areas have one or two layers of cells. The area, which has four or five layers, develops into the anterior end of the larva. High power light microscopy revealed three types of cells according to morphological and staining properties.

Type one cells, the major cell type of this stage, are spherical, and each contains a nucleus which has a prominent, centrally-located nucleolus (Fig. 2). With polychrome stain, the nucleus is stained more lightly than the cytoplasm. Some type one cells which are present at the anterior end, are smaller than the type one cells in the remaining areas. The type one cells probably represent undifferentiated cells.

Type two cells, the darkest staining cells of the three cell types, are irregularly-shaped, with wide cytoplasmic processes (Fig. 3). These processes range in the intercellular spaces among type one cells, and

they are always in contact with the tegument. The nuclei of type two cells are obscured because of the low contrast between nuclear and cytoplasmic constituents.

Type three cells, which represent the lightest staining cells, are large and spindle-shaped and lack cytoplasmic processes (Fig. 4). Their nuclei, as with type one cell nuclei, are more lightly stained than the cytoplasm. A small nucleolus also is present in the nucleus. Type three cells are the least numerous in stage two larvae.

B. Stage Three Larvae:

Stage three larvae were obtained from beetles eight to nine days after experimental infection. Cells begin to proliferate rapidly at the anterior end of a stage two larva. In time, the entire larva becomes elongated and doubles in size. Thus, numerous layers of cells are present at the anterior end, and the central cavity of the larva is enlarged and eccentric. Further growth and elongation of the stage two larva result in a stage three larva which has three body divisions: forebody, midbody, and hindbody. Few beetle haemocytes are attached to the stage three larva. While the brush borders of the midbody and hindbody are well developed, the brush border of the forebody is poorly developed. However, the tegument of the forebody is thicker than the tegument of the midbody and hindbody.

The forebody is a round, solid structure which will develop into the scolex of the cysticercoid. Cross sections of the forebody are tetra-lobate (Fig. 5). Cells are densely packed into five clusters, four clusters located in each of the lobes and one cluster in the center of the section. Type three cells and type two cells are the major cell

types of the forebody. Few type one cells are present. Type three cells and type two cells are aggregated and aligned in each of the four lobes from which the future suckers of the scolex will develop (Fig. 6). Here, a layer which forms the inner border of the rudimentary sucker, begins to develop. The musculature of the rudimentary suckers is poorly developed. A new cell type, which will be designated as a type four cell, is present in intercellular spaces between the aforementioned five clusters (Fig. 7). The type four cell is roughly star-shaped with five or six branched cytoplasmic processes whose structure resembles the processes of a multipolar neuron. A prominent nucleolus is present in the center of each nucleus, which again is less dense than the surrounding cytoplasm.

At the transitional zone between the forebody and midbody, both type one and type two cells are interspersed around its periphery and form a loose cellular layer beneath the tegument (Fig. 8). Clusters of type three cells and elongated type one cells are present in the subtegmentary cell layer (Fig. 9). Type four cells have highly branched cytoplasmic processes which connect with one another and form a loose network in the middle of the larva (Fig. 10). The formation of calcareous corpuscles can be detected in some type four cells of this region (Fig. 11).

The midbody is the longest and the thickest division of the stage three larva, the major portion of which is ovoid and contains a round, centrally-located cavity (Fig. 12). A subtegmentary cellular layer consists of type two cells and a fifth cell type, type five cell, which presumably is derived from type one cells. The developing type five cells become aligned with their long axis perpendicular to the tegument.

Type five cells are lightly-stained, pear-shaped cells, with a vesiculated cytoplasm and a nucleus with one prominent nucleolus (Fig. 13). These cells resemble type one cells, except for their staining properties and vesiculated cytoplasm.

The central cavity of the midbody of this stage is surrounded by both outer and inner concentrically-arranged fibrous layers (Fig. 12). A wide space separates the outer from the inner fibrous layer, but they unite with each other at the anterior and posterior ends of the midbody. The outer fibrous layer and the subtegumentary layer eventually develop into the wall of the capsule. The outer fibrous layers are composed chiefly of a new cell type, type six cell, which is spindle-shaped and stained darkly with large nucleus which contains a prominent nucleolus. These cells also bear long cytoplasmic processes (Fig. 14).

The hindbody, which develops into the tail, is a round, solid structure (Fig. 15). The anterior end of the hindbody consists of cell types one, two, five and six. Type two and type five cells form the subtegumentary cellular layer of the hindbody. Type one and type six cells form the core of the hindbody (Fig. 16, 17). Type five cells decrease in number while the hindbody decreases in diameter posteriorly.

C. Stage four and stage five larvae:

As development of stage three larvae continues, the body becomes further elongated; and a constriction forms between the forebody and the midbody. Incompletely developed suckers also become recognizable as development proceeds. When a stage three larva reaches this degree of complexity, invagination of the scolex begins. The scolex is withdrawn into the central cavity of the midbody while the partially developed outer and inner capsule fold-over anteriorly such that only

a narrow passage, the anterior canal, remains in communication with the exterior. Larvae with withdrawn scoleces are designated as stage four larvae.

Stage four larvae were obtained from beetles ten days after experimental infection. The stage four larva has an ovoid-shaped body, which contains the invaginated scolex, and a round, slender tail. The scolex has no significant changes in comparison with that of the late stage three larva. The capsule, which surrounds the scolex, resembles the midbody of the stage three larva.

There is no dramatic change in body shape when stage four larvae develop into stage five larvae. Stage five larvae were obtained from beetles eleven days after experimental infection. Both body and tail of stage five larvae are covered with a well developed brush border.

The anterior canal of stage five larva is reduced to a blind slit in the center of the body, between the dorsal and the ventral sides. The opening of the anterior canal is broad and voluminous (Fig. 18). From the opening, the anterior canal steadily narrows posteriorly where the canal walls unite, forming a plug which occludes the canal (Fig. 19, 20). The anterior canal is lined with tegument. The subtegumentary cellular layer of the anterior canal consists mainly of type five cells with a few type two cells interspersed in them (Fig. 19). The plug, which is connected with the scolex, is composed of parenchymal cells embedded in an amorphous jelly-like substance and is surrounded by a fibrous layer of type six cells (Fig. 22). Parenchymal cells probably derived from type one cells.

The invaginated scolex, which is connected to the body by a slender, basal stalk, is composed of parenchymal and muscle cells and has four

well developed suckers (Fig. 22). The muscle cells of the suckers are well developed and are aligned with their long axes perpendicular to the surface (Fig. 23). The musculature and the inner border of the suckers are well developed in this stage. Sections, which were cut through the invaginated scolices, have many spaces of varying sizes. These spaces represent calcareous corpuscles which have probably been removed during sectioning. Calcareous corpuscles are especially numerous at the anterior and posterior ends of the invaginated scolex (Fig. 24).

The outermost layer of the stage five larval capsule is a tegument with a brush border. Beneath the tegument is a subtegumentary cellular layer (which is termed the intermediate layer by other investigators) of elongated type five cells, with some type two cells interspersed in them (Fig. 25). Type five cells are much more orderly aligned and contain many more vesicles in their cytoplasm than type five cells of the stage three larvae.

A fibrous layer with numerous intercellular spaces, especially about the lateral sides of the larva (Fig. 26), underlies the subtegumentary cellular layer. Typical type six cells are found in the outer portion of the fibrous layer but toward the inner portion of the larva, they become elongated, and their cytoplasm stains intensely. These morphological changes, and the close association between type six cells and the fibers, suggest that the type six cells are involved in the formation of fibers. The fibrous layer overlies a dense fibrous layer and is separated from it by a thin layer of densely-packed, darkly stained fibers (Fig. 26). The dense fibrous layer is composed of fine, densely-packed, concentrically oriented fibers and of a few

type six cells.

A densely stained cellular layer which is underneath the dense fibrous layer, surrounds and is connected to the invaginated scolex by a slender basal stalk. This layer comprises small, light-stained parenchymal cells within a very dense-stained ground substance.

The subtegumentary cellular layer of the tail comprises type two cells, type three cells, type four cells and their cytoplasmic processes. The middle of the tail consists of type one cells and type four cells with branched cytoplasmic processes.

II. Electron Microscopy:

A. Stage Two Larvae:

The free surfaces of stage two larvae are composed of numerous long, fine cellular projections which arise from the tagument (Fig. 34). These projections are limited by an outer plasma membrane and are similar to the microvillar extensions in other cells. The matrices of individual microvilli lack filaments and contain an amorphous substance. The microvilli are extremely long, branched, and densely-packed in the areas where beetle haemocytes are attached. Some microvilli in these areas often have dilated regions (vesicles) at their tips, which are less electron-dense than remaining portions of the microvilli (Fig. 29). Some vesicles are in contact with the cell membrane of beetle haemocytes.

Beetle haemocytes are in close contact with one another and generally several occur in chains which are attached to the larval microvilli at their long sides (Fig. 30). Each spindle-shaped haemocyte contains a single ovoid-shaped nucleus with one electron-lucent

nucleolus and a large amount of euchromatin and only a narrow rim of heterochromatin adjacent to the nuclear membrane. Haemocytes contain numerous free ribosomes, few profiles of granular endoplasmic reticulum, mitochondria, many lipid droplets and numerous primary and secondary lysosomes (Fig. 31). Many phagocytic vacuoles lined with microvilli occur in the haemocytes, but only along the sides which are in direct contact with the haemocytes (Fig. 29).

Some haemocytes, attached to the late stage two larvae, undergo degradative reactions. The initial degradative changes include condensation of the chromatin in the nucleus, an increase of phago-lysosomal vacuoles, and of lipid droplets in the cytoplasm (Fig. 32). Late in the course of degradation, the chromatin of the nucleus is extremely clumped (pyknosis) and organelles have completely dissolved (Fig. 33). Thus, haemocytes in the late degradative stage are lightly stained and have pyknotic nuclei.

The tegument of second stage larvae is a thin, un-nucleated, syncytial layer, which is connected to subtegumentary cells (which represent the nucleated cell bodies of the tegument) by many long, tenuous cytoplasmic processes (Fig. 34). (Subtegumentary cells are designated as type two cells in the results based on light microscopic observation.) Subtegumentary cells located beneath a muscle layer are electron-dense and irregular in shape, with many slender cytoplasmic processes and some being binucleate (Fig. 35). The nucleus of the subtegumentary cell is irregular in shape with a large nucleolus. The nuclear envelope has several deep indentations. The karyoplasm is not as electron-dense as the cytoplasm since it does not contain condensed chromatin. Numerous beta glycogen granules and vesicles of varying sizes are

predominant features of the cytoplasm. The cytoplasm also contains electron dense granules, large mitochondria and smooth endoplasmic reticulum.

The tegument of stage two larvae is approximately 0.3 μm . in thickness. There is considerable variation in the thickness of the tegument since both the outer and inner membranes are irregular (Fig. 36). The inner membrane has more folds than the outer limiting membrane and closely follows the contours of the underlying muscle fibers. The ground substance of the tegument consists of a few beta glycogen granules, mitochondria, and vacuoles.

The subtegumentary circular muscle bundles and their cell bodies are scattered beneath the tegument and between subtegumentary cells. (The cell bodies of muscle cells were designated as type three cells in the light microscopic results.) The nucleus, which is located within the cell body, is electron-lucent since it only contains euchromatin and is enveloped by a double membrane (Fig. 36). The outer membrane of the nuclear envelope is studded with ribosomes. The perinuclear sarcoplasm contains granular endoplasmic reticulum, mitochondria, a few dilated cisternae with moderate electron-dense amorphous material, numerous free ribosomes, and beta glycogen. The long, thick cytoplasmic processes of muscle cells contain the myofilaments, which appear to be non-striated with an irregular arrangement of both thick and thin myofilaments running parallel with one another (Fig. 37). The cytoplasmic processes also contain a considerable amount of free ribosomes and beta glycogen aggregations forming clusters.

Beneath the circular muscle layer is an irregularly-arranged subtegumentary cellular layer which consists mainly of type one cells

interspersed with some subtegenentary cells (Fig. 38). The cellular layer is separated from the central cavity at the anterior end of the larva by several layers of thin cytoplasmic processes. There is no boundary between the cellular layer and the central cavity in the remaining areas. The type one cell of the subtegenentary layer is irregularly shaped with a large electron-lucent nucleus containing a large electron-dense nucleolus. The cytoplasm is filled with free ribosomes and it also contains mitochondria, rough endoplasmic reticulum, and beta glycogen granules (Fig. 39).

Larval hooks containing of a blade, a guard, and a handle are attached to the posterior end of the stage two larvae (Fig. 40). The handle is inserted into the cellular layer and the blade and the guard protrude out from the surface of the larva. The ball-shaped base of the handle is embedded into the cup-shaped socket of electron-dense material to which muscles attach (Fig. 41). Fibrillar elements connect the ball-shaped base to the cup-shaped socket. Myofilaments in the muscles which attach to the socket gradually decompose leaving an area which contains aggregated, amorphous ground substance (Fig. 42). The cross sections of the larval hooks consist of an electron-opaque outer granular layer, a middle fibrous layer, and a central core (Fig. 43).

B. Stage Three Larvae:

Fewer beetle haemocytes are attached to stage three larvae than the previous stage. They are fastened to the stage three larvae individually and do not connect as a chain. The ultrastructure of haemocytes does not differ from that of the haemocytes of stage two larvae.

The forebody: The ultrastructure of the tegument in the forebody of stage three larvae differs from the tegument of stage two larvae, and

also from the tegument of the midbody and hindbody of the stage three larvae. Besides microvilli, additional cellular projections, microtriches, begin to form on the free surface of the tegument (Fig. 44). The tegument begins to shed its microvilli when microtriches begin to form. An individual microtrich is a short, thick cellular projection with a conical electron-dense tip and a less-dense proximal part. The tegument also increases in thickness and contains, in addition to beta glycogen granules and mitochondria, many vacuoles and electron-dense granules which are surrounded by electron-translucent spaces. In some areas, the tegument sinks into the muscle layer and forms tegumentary invaginations (Fig. 45).

The subtegumentary circular muscle layer of stage three larvae is thicker than the corresponding muscle layer of stage two larvae and the cytoplasmic extensions (Fig. 45), contain more myofilaments than those of stage two larvae (Fig. 45). Small electron-dense rectangular-shaped bodies (dense bodies) occur among the myofilaments (Fig. 46). These apparent morphological changes in muscle cells from stage two to stage three larvae suggest that these cells undergo further differentiation.

Beneath the muscle layer is the medullary region of the forebody which consists of a variety of cell types which are very densely-packed (Fig. 47). Type one and muscle cell bodies, which underlie the subtegumentary muscle layer are not ultrastructurally different from those of stage two larvae. In addition to the organelles present in this region of stage two larvae, the subtegumentary cells contain

electron-dense granules surrounded by electron-transparent spaces similar to those in the tegument section (Fig. 47).

The medullary region of the rudimentary suckers, described previously in light microscope observations, is comprised mainly of muscle cells. Muscle cells which form clusters at the middle of the rudimentary suckers, often appear to connect with one another by their cytoplasmic strands and to form a multinuclear cell, which probably is the result of several nuclear divisions without cytoplasmic division, and have large nuclei with electron-opaque nucleoli (Fig. 48). Their sarcoplasm contains a few myofilaments, some beta glycogen granules, vacuoles, several mitochondria containing moderate dense matrices, and numerous ribosomes.

The transitional zone: The tegument and its microvilli of the transitional zone between the larval forebody and midbody undergo no significant changes from those of stage two larvae. The subtegumentary muscle layer is thicker than that of stage two larvae. The muscle cells also undergo further development as previously mentioned. The loosely arranged subtegumentary cellular layer which is beneath the muscle layer consists of a variety of cell types. The ultrastructures of subtegumentary cells and of most type one cells do not differ from those of stage two larvae. But some type one cells, which are located in the innermost layer of the subtegumentary cellular layer, have begun to develop into a protonephridial system.

The terminal organ of the protonephridial system develops from two type one cells. Two adjacent type one cells elongate and

become spindle-shaped (Fig. 49). Their nuclei are similar to those of typical type one cells, but their cytoplasm undergoes dramatic changes. The cytoplasm consists of numerous polysomes, microtubules, and mitochondria (Fig. 50, 52). One of the two developing type one cells, the nephridial funnel cell, contains several vacuoles of varying sizes in the cytoplasm. Gradually, these vacuoles coalesce and form a funnel-shaped nephridial tubule at the end of the nephridial cell. A circle of approximately six finger-like cytoplasmic projections (nephridial cell rods) arises from the opening of the funnel-shaped tubule of the nephridial funnel cell (Fig. 50). Besides the nephridial cell rods, the nephridial funnel cell also has thin, cytoplasmic processes. The other developing type one cell (the flame cell) begins to form flagella. The end which bears flagella contains more microtubules, but it contains fewer polysomes than the remaining areas.

The flame cells of this stage have about 17 circular flagella at their basal regions (Fig. 50). The flagella, which compose the flame of the terminal organ, are loosely packed in the terminal organ. Flagella are round in cross-section and have the typical nine-plus-two arrangement of axial filaments with basal bodies inserting into the cytoplasm. In a given flame, not all are the central pairs of axial filaments aligned in the same direction (Fig. 50). A circle of approximately eight finger-like projections (flame cell rods) arises from the cytoplasm of the flame cell. Several tenuous cytoplasmic projections, which Kunnel (1964) termed leptotriches, arise from the inner wall of each flame cell rod. Desmosome-like structures run along the

whole length of each interdigitating contiguous surface rather like a zipper (Fig. 51). Consequently, the flame cell connects with the nephridial cell; and a funnel-shaped tubule, which houses a tuft of flagella, is constructed between these two cells (Fig. 52). Therefore, cross sections which are cut through the interdigitating area of a nephridial tubule contain a flame which is surrounded by inner flame cell rods and outer nephridial cell rods (Fig. 50). The gaps between the adjacent interdigitating rods are filled with material of desomsome-like appearance. In cross section, the interdigitating region of the nephridial tubule is approximately 2.5 μm . in diameter.

Collecting ducts of the protonephridial system are found adjacent to the terminal organs. Collecting ducts are intracellular and are surrounded by cytoplasm which contains mitochondria, microtubules, free ribosomes and vesicles (Fig. 53). The ovoid-shaped nucleus of each collecting duct consists of a large nucleolus and a narrow rim of heterochromatin adjacent to the nuclear membrane. The collecting duct cell has several thick cytoplasmic processes. The surface of the collecting duct lumen has several thin cytoplasmic processes.

The middle portion of the transitional zone consists mainly of type four cells and their highly branched cytoplasmic processes. Each type four cell has a large, irregular-shaped nucleus with an eccentrically-located nucleolus (Fig. 54). The nucleus is electron-lucent because it is composed mainly of euchromatin. The perinuclear cytoplasm contains numerous free ribosomes, rough endoplasmic reticulum, and several mitochondria (Fig. 55). The highly branched cytoplasmic processes are studded with beta glycogen granules. Mitochondria are located in the larger cytoplasmic branches. The fine branches of the

cytoplasmic processes are generally in close contact with other types of cells (Fig. 56).

The calcareous corpuscles begin to form in stage three larvae. Cells in various stages of calcareous corpuscle formation were found throughout the middle portion of the transitional zone and were most abundant in the marginal regions of the middle portion. The cells in which calcareous corpuscles are formed are generally surrounded by fine cytoplasmic branches of type four cells (Fig. 57). The nuclei of calcareous formation cells are oval in young cells, but are cup shaped and displaced to one corner by a large calcareous corpuscle in mature cells. The nuclei of young cells contain large amounts of euchromatin, ribosome-like granules, and only a narrow rim of heterochromatin near the nuclear membrane (Fig. 59). One nucleolus is always present. Nuclei are rather electron-dense since they contain numerous ribosome-like granules. The cytoplasm forms a thin sheath around the calcareous corpuscle, but a relatively large volume of it is concentrated around the nucleus. The cytoplasm consists of free ribosomes and mitochondria, but more free ribosomes are present in the perinuclear cytoplasm than in remaining areas. The calcareous corpuscles vary in size and shape and their densities depend on which stage of calcareous corpuscle formation they are in. A thin membrane separates the calcareous corpuscle from the cytoplasmic matrix. The membranes bordering old calcareous corpuscles have numerous, vermiform cytoplasmic folds which project into the cavity containing the calcareous corpuscle (Fig. 58). A young calcareous corpuscle has an irregularly-shaped, electron-dense center which is surrounded by homogeneous matrix. In addition, electron-dense margins stud the calcareous corpuscle membrane (Fig. 59). The fine granules of the homogeneous

matrices do not resemble crystalline elements found in other substances which undergo calcification, such as bone and tooth. The fine granules are evenly distributed in young calcareous corpuscles and gradually, with time, these granules accumulate around the dense centers. Thus, the peripheral scope of the dense centers gradually increases (Fig. 58). Granules also aggregate in small electron-dense patches at peripheral areas. Occasionally, small vacuoles are found in the calcareous corpuscles.

The Midbody: The tegument in the midbody of stage three larvae does not significantly differ from that of stage two larvae. The muscle layer is thicker than the corresponding muscle layer of stage two larvae. The myofilaments in the cytoplasmic extensions of the muscle cells undergo differentiation similar to that of the myofilaments in the forebody. The ultrastructure of muscle cell bodies is modified slightly. The perinuclear sarcoplasm of the large muscle cells consists of numerous dilated cisternae of rough endoplasmic reticulum which contain moderately-dense substance, polyribosomes, and several mitochondria with electron-dense matrices (Fig. 60).

In addition to the subtegumentary cells and muscle cells, the subtegumentary cellular layer is comprised mainly of cell types one, and five. The subtegumentary cells of stage three larvae undergo no prominent changes from stage two larvae. Type five cells which are derived from type one cells are the principal cell type of the subtegumentary cellular layer. Type one cells in the peripheral area of the subtegumentary cellular layer of young stage three larvae elongate and become aligned themselves with their long axes perpendicular to the tegument. Simultaneously, these type one cells begin to

differentiate into type five cells. The cytoplasm of young differentiating type one cells includes mitochondria, free ribosomes, and rough endoplasmic reticulum with dilated electron-translucent cisternae. The dilated cisternae of rough endoplasmic reticulum serve as an indicator of the differentiating stages of type one cells; more dilated cisternae are found in old type one cells than in young type one cells. (Old type one cells are termed type five cells.) Type five cells of stage three larvae are pear-shaped with an ovoid, electron-lucent nucleus containing a single nucleolus (Fig. 61). The outer nuclear envelope is studded with ribosomes. The cytoplasm contains numerous free ribosomes, several mitochondria, and rough endoplasmic reticulum with dilated cisternae containing moderately-dense substance.

Some type one cells gradually develop into type six cells in the zone between the subtegumentary cellular layer and the outer fibrous layer. These developing type six cells in the outer portion of the outer fibrous layer start to elongate and lipid droplets of various sizes begin to form in the perinuclear cytoplasm (Fig. 62). The cell bodies of these cells in the inner portion of the outer fibrous layer become spindle shaped with long, thin cytoplasmic processes within an amorphous extracellular ground substance filled with fibrils. In the outer fibrous layer, the distal cytoplasmic processes of these cells further elongate; and additional extracellular ground substance and fibrils accumulate. The thin extremely long cytoplasmic processes of type six cell make up the fibrous elements of the outer fibrous layer.

The fibrous elements are concentrically arranged in the outer fibrous layer. The type six cell has an ovoid nucleus with an eccentric nucleolus (Fig. 63). The perinuclear cytoplasm contains lipid droplets

of varying sizes, mitochondria, free ribosomes, and rough endoplasmic reticulum. The thin, extremely long cytoplasmic processes which follow the contour of the outer fibrous layer contain small lipid droplets, free ribosomes, and rough endoplasmic reticulum.

The inner fibrous layer is composed of type four cells and their highly branched cytoplasmic processes. Type four cells of stage three larvae resemble those of stage two larvae except that the former bear more branched cytoplasmic processes than the latter (Fig. 64). These highly branched cytoplasmic processes contact one another and form the dense network of fibrous elements found in the inner fibrous layer.

C. Stage Four (10-day-old) Larvae and Stage Five (over 12-day-old) Larvae

Several beetle haemocytes often attach to the surface of stage four and five larvae. The tegument of stage four larvae with newly invaginated scolices differs little from that of stage three larvae. The tegument grows in thickness and undergoes tremendous morphological modifications when stage five larvae grow old. The tegument is the outer-most layer of the capsule of mature cysticercoids.

The tegument of 23-day-old larvae is 3.0 μm . and it is 10 times thicker than the tegument of stage two larvae. Materials are gradually added to the tegument during the course of development by subtegumentary cells (the cell bodies of the syncytial tegument). A thin, but irregular, electron-dense zone divides the 23-day-old tegument into two layers, the distal layer and the proximal layer (Fig. 65, 67). The distal layer contains numerous, small, uniform vesicles; and the proximal layer contains numerous, large, vesicles of varying sizes and

mitochondria. Several large, round vesicles with irregularly-shaped, electron-opaque cores are interspersed in both layers. In some areas, the tegumentary surface swells and forms several huge vesicles in a manner similar to a blister. These huge vesicles are probably the result of the coalescence or condensation of many smaller vesicles which are presented in the tegument (Fig. 66).

A notable change in the subtegumentary cellular layer of stage five larvae is the presence of an extracellular ground substance. Fibrils accumulate in the extracellular ground substance during the course of development, and eventually they become the predominant component. The fibrils are arranged circularly in the outer region, longitudinally in the middle region, and irregularly in the inner region (Fig. 66). Muscle bundles, which are dispersed throughout the outer region of the subtegumentary cellular layer, are embedded in the fine, circularly-arranged fibrillar ground substance. The ultrastructure of muscle extensions is similar to that of stage three larvae.

Cells are loosely dispersed in the subtegumentary cellular layer in contrast to the condition in stage three larvae (Fig. 67). Type five cells are the principal cells of this layer but are interspersed with subtegumentary cells. The subtegumentary cell of the 23-day-old larva has an irregularly-shaped nucleus with a large nucleolus and a narrow rim of heterochromatin adjacent to the nuclear membrane (Fig. 67). The nuclear cytoplasmic ratio decreases, probably due to nuclear shrinkage and/or cytoplasmic increase. In addition to mitochondria, free ribosomes, and large, round vesicles with irregular, electron-dense cores, a great many vesicles of varying sizes also occur in the cytoplasm.

The major ultrastructural change in type five cells of stage five larvae is the development of additional dilated cisternae containing electron-lucent material (Fig. 68). Rough endoplasmic reticulum and their dilated cisternae are the predominant organelles of type five cells. The membranes of some dilated cisternae often unite with the cell membrane. Mitochondria and free ribosomes are present in the cytoplasm. The nucleus of the type five cell contains a nucleolus and a narrow rim of heterochromatin. The distal ends of pear-shaped type five cells are elongated and form narrow cytoplasmic processes which reach to the bottom of the tegument (Fig. 68). These cytoplasmic processes do not contain dilated cisternae.

A new layer, the loose fibrous layer, is formed in stage five larvae. The loose fibrous layer, which is beneath the subtegumentary cellular layer, consists of numerous circular arranged fibers and fine cytoplasmic processes (Fig. 69). The fibrous bundles are composed of numerous fibrils which are similar to that of the subtegumentary cellular layer.

The terminal organs of the protonephridial system are embedded in the outer region of the loose fibrous layer. The terminal organs of 23-day-old larvae increase in size and complexity in contrast to those of stage three larvae. The ultrastructure of the flame cells and the nephridial funnel cells in 23-day-old larvae are quite different from those in stage three larvae. Flame cells stain very lightly because both nuclei and cytoplasm are highly vacuolated (Fig. 70). The irregularly-shaped nucleus contains scattered heterochromatin and also a thin rim of heterochromatin studs the nuclear envelope. The cytoplasm contains free ribosomes, many microtubules, several

mitochondria with electron-dense matrices, and many vesicles of varying sizes. The flame cell bears a circle of approximately 23 flame cell rods which interdigitate with nephridial funnel rods (Fig. 71). The nuclei of the nephridial funnel cells undergo changes similar to the nuclei of the flame cells. The nucleus of the nephridial funnel cell is surrounded by a thin rim of cytoplasm which contains mitochondria, free ribosomes, microtubules, and small vesicles (Fig. 72). The cytoplasm of the funnel-shaped tubule also contains the aforementioned organelles. The nephridial funnel cell has a circle of approximately 22 nephridial funnel rods (Fig. 70).

In cross section, the flame of the terminal organ is ovoid and contains about 36 densely packed flagella at the interdigitated region of the funnel-shaped nephridial tubule (Fig. 71). Adjacent flagella are separated from each other by a gap which is filled with amorphous, moderate-dense material. The flame of stage five larvae has approximately two times more flagella than the flame of stage three larvae. In a given flame all of the central pairs of axial filaments are arranged in the same direction. Flagella are hexagonal in shape except the peripheral flagella. Each side of the flagellum is in contact with another flagellum. Thus, each flagellum, with the exception of the peripheral flagella, is surrounded by six other flagella. The flagella vary in length, and about one third of them extend to the tip of the flame (Fig. 72).

The funnel-shaped nephridial tubules, which contain the flames, are approximately 3.0 μm . in diameter at the interdigitated region, and are about 1.2 times larger in diameter than those of stage three larvae. Nephridial tubules are composed of 23 flame cell rods which

mitochondria with electron-dense matrices, and many vesicles of varying sizes. The flame cell bears a circle of approximately 23 flame cell rods which interdigitate with nephridial funnel rods (Fig. 71). The nuclei of the nephridial funnel cells undergo changes similar to the nuclei of the flame cells. The nucleus of the nephridial funnel cell is surrounded by a thin rim of cytoplasm which contains mitochondria, free ribosomes, microtubules, and small vesicles (Fig. 72). The cytoplasm of the funnel-shaped tubule also contains the aforementioned organelles. The nephridial funnel cell has a circle of approximately 22 nephridial funnel rods (Fig. 70).

In cross section, the flame of the terminal organ is ovoid and contains about 36 densely packed flagella at the interdigitated region of the funnel-shaped nephridial tubule (Fig. 71). Adjacent flagella are separated from each other by a gap which is filled with amorphous, moderate-dense material. The flame of stage five larvae has approximately two times more flagella than the flame of stage three larvae. In a given flame all of the central pairs of axial filaments are arranged in the same direction. Flagella are hexagonal in shape except the peripheral flagella. Each side of the flagellum is in contact with another flagellum. Thus, each flagellum, with the exception of the peripheral flagella, is surrounded by six other flagella. The flagella vary in length, and about one third of them extend to the tip of the flame (Fig. 72).

The funnel-shaped nephridial tubules, which contain the flames, are approximately 3.0 μm . in diameter at the interdigitated region, and are about 1.2 times larger in diameter than those of stage three larvae. Nephridial tubules are composed of 23 flame cell rods which

interdigitate with 22 nephridial funnel rods. The flame in this area contains approximately 36 flagella. The nephridial tubule decreases in diameter toward the end of the nephridial funnel cell body. The narrow end of the nephridial tubule is 0.9 μm . in diameter and the flame at this end contains about 13 flagella (Fig. 72).

The dense fibrous layer, which underlies the loose fibrous layer, consists of circularly-arranged, attenuated cytoplasmic processes from bipolar-shaped type six cells (Fig. 73). These thin cytoplasmic processes are very densely packed and are embedded in an extracellular fibrillar ground substance. Type six cells of 23-day-old larvae are elongated. The nuclei of type six cells are sausage-shaped and each contains a nucleolus. The nucleus is surrounded by a thin rim of cytoplasm. Type six cells in stage five larvae undergo no prominent ultrastructural changes from those of stage three larvae.

Collecting ducts of the protonephridial system are found between the loose and the dense fibrous layers of stage five larvae. The ultrastructure of the collecting duct differs from that of stage three larvae. The cytoplasm, which surrounds the collecting duct, contains mitochondria, free ribosomes, small vesicles and melanin-like granules (Fig. 74). The nucleus of the collecting duct cell contains a nucleolus, scattered heterochromatin, and a thin rim of heterochromatin about the nuclear membrane. The surface of the collecting duct lumen varies in sizes and is lined with bead-like cytoplasmic processes. Occasionally, two ducts are found in a single cell.

A dense cellular layer overlies the invaginated scolex. A narrow gap, filled with vesicles and a moderate-dense substance, separates the dense cellular layer from the invaginated scolex (Fig. 75).

However, a slender stalk connects this layer to the basal part of the invaginated scolex. Thus, this layer is continuous with the invaginated scolex. The free surfaces of the dense cellular layer and the invaginated scolex are composed of numerous microtriches, but the free surface of the scolex has more microtriches than that of the dense cellular layer. Parenchymal cells and their cytoplasmic processes are the principal cells of the dense cellular layer (Fig. 76). The ultrastructure of parenchymal cells resembles type one cells. The cytoplasmic processes of parenchymal cells are filled with beta glycogen granules and mitochondria. The terminal organs and collecting ducts are also found in this layer.

In stage five larvae, many parenchymal cells are engaged in forming calcareous corpuscles. Some areas in the dense cellular layer of 23-day-old larvae are filled with huge calcareous corpuscles (Fig. 77) which are removed during sectioning probably because of their hardness or possibly because of poor penetration of the embedding medium. Parenchymal cells containing corpuscles become expended themselves and atrophy. Their nuclei become pyknotic, and their cytoplasm becomes extremely thin and contains few recognizable organelles (Fig. 78).

The outer limiting membrane of the tegument of the invaginated scolex extends into numerous microtriches, which resemble those described for stage three larvae (Fig 76). The tegument contains vesicles surrounded by an amorphous electron-dense substance and melanin-like granules (Fig. 79). As stage four larvae develop and mature to stage five larvae, the tegument becomes increasingly vesiculated. The

inner membrane develops many folds and closely contacts the subtegumentary muscle layer.

The subtegumentary muscle layer is very well developed in 23-day-old larvae. The muscle layer is thicker in the suckers than in the inter-sucker regions. Muscle bundles extend in different directions in the scolex. Some muscle bundles penetrate deeply into the medullary region of the scolex (Fig. 80).

Beneath the subtegumentary muscle layer is a medullary region of the scolex, which consists of various cell types (Fig. 81). Subtegumentary cells and muscle cell bodies are located about the periphery, and both cells undergo ultrastructural change similar to that of cells in the capsule. Terminal organs and parenchymal cells are also found in the medullary region.

The invaginated scolex of the 23-day-old larva communicates with the exterior by an anterior canal. The anterior canal is lined with a tegument which bears numerous long microvilli on its free surface (Fig. 82). It is difficult to trace a given microvillus from its origin to its terminus because the microvilli contact one another and form a dense network in the anterior canal. The anterior canal is occluded by a plug which is connected to the scolex. The plug consists of parenchymal cells, collecting ducts, and numerous cytoplasmic processes (Fig. 83). Many parenchymal cells, are engaged in the formation of calcareous corpuscles as are cells in the dense cellular layer of the capsule.

DISCUSSION

The rate of postembryonic development of the tapeworm, Hymenolepis diminuta, in the intermediate host, Tribolium confusum, which were maintained 30°C, has been established by Voge and Heyneman (1957) and Rothman (1957). During the course of the present study, grain beetles, Tenebrio molitor, served as intermediate hosts for H. diminuta and were kept at 25°C. Although the rate of the postembryonic development is affected by using a different host which is kept at lower temperature, the basic pattern of postembryonic development is not affected. Obviously, the rate of development is closely correlated with the temperature within a certain range (15°C to 35°C) at which the host are maintained. In this research it took two more days to reach each developmental stage at 25°C than at 30°C (Fig. 84).

Stage five larvae of H. diminuta reach the infective stage on the fourteenth day after experimental infection. The light and electron microscopy studies of stage five larvae also confirmed that the invaginated scolices reach full development about fourteen days post-infection. Therefore, the scolices of stage five larvae do not change significantly beyond the fourteenth day. However, the capsules surrounding the invaginated scolices begin to differentiate in late stage three larvae, and the development continues through the late stage five larvae and undergoes the greatest degree of change in stage five.

The interactions of haemocytes of T. confusum and cysticercoids were studied by Ubelaker et al (1970b) and Collin (1970). Ubelaker's

observations were based on 8-day-old cysticercoids (stage five larvae) of Hymenelepis diminuta. He described microvilli of cysticercoids which were surrounded by host haemocytes. He suggested a possible defensive mechanism of cysticercoids to host haemocytes. Collin reported the interactions of host haemocytes and cysticercoids of H. cetelli in which the 3-day-old cysticercoids were surrounded by one to four layers of haemocytes and 5-day-old ones were surrounded by a few cytolysed haemocytes. The comparison of the above observations with this report reveals several differences. Generally, only a single layer of haemocytes attach on stage two and three larvae. More cytolysed haemocytes are found attached to stage three larvae than stage two larvae. It appears that cytolysed haemocytes break loose from cysticercoids and are not replaced by new haemocytes. The new methods of study, including immunological studies, are needed to clarify these host-parasite interactions. The differences between the present study and the earlier investigations may be due to: (1) different host and parasite, (2) cysticercoids of various ages.

Several investigators have attempted to identify the germinative cells from hatched oncospheres or early cysticercoids. Rybicka (1966) demonstrated that the first several cleavages of embryogenesis in H. diminuta are assymetric divisions giving rise to the macromeres, mesomeres, and micromeres. She suggested that germinative cells arise from mesomeres during early embryonic development. She described the germinative cells as having huge nuclei with conspicuous nucleoli and having scant cytoplasm rich in ribonuclear acid. Ogren (1962) indicated that the first germinative cells of H. diminuta arose from the

original epidermal gland cells. He described the germinative cells as having large nuclei with large nucleoli and cytoplasm rich in ribonuclear acid. Collin (1968) demonstrated that the germinative cells of Hymenolepis citelli are not a part of the epidermal gland but that they lie next to it. He reported that a hatched oncosphere consists of muscle cells, and cells of type one, two, and three. He suggested that type two cells are germinative cells. Type one cells in this report ultrastructurally resemble the germinative cells described by Rybicka (1966), Collin (1968), and Ogren (1962). The type one cells probably arise from the germinative cells which were described by these investigators during the early postembryonic development. The ultrastructure of the type one cells is relatively undifferentiated. Therefore, the type one cells presumably are the primordial cells of the postembryonic development.

Rybicka (1973) studied the origin and differentiation of the tegument of preoncospheres. She identified a binucleate cell which is the cell body of the tegument in the center of the preoncosphere of Hymenolepis diminuta. She suggested a continuity in the development of cestode tegument in the embryonic, larvae and the adult cestode. The tegument of stage two larvae in this report is the result of further growth and differentiation of the subtegumentary cells of oncospheres. The tegument of stage three larvae begins to show differential development of various parts of the body. The free surface of the forebody begins to form microtriches, whereas the free surface of the capsular wall remains the same as in the early larval stages. The ultrastructure of the tegument of the invaginated scolices does not change significantly

when the development proceeds. However, the tegument of the capsules undergoes a prominent differentiation and development continues through late stage five larvae. Therefore, the ultrastructure of the capsular tegument changes greatly from early stage four larvae to late stage five larvae.

The capsular tegument differs from that described by Ubelaker et al (1970a) because their report is based on 8-day-old larvae (early stage five larvae). The capsular tegument of the present study became vesiculated as the development proceeds. In addition, the tegument of 23-day-old larvae consists of a thin distal layer and a thick proximal layer and huge vesicles are found on the free surface of the tegument. Microvilli occur in the inner surface of some of these vesicles. Secretory granules or matrices are not found in any of these vesicles. These vesicles ultrastructurally resemble the ballooning structures on the tegument of a hatched oncosphere of Hymenolepis citelli (Collin, 1968). Rybicka (1973) pointed out that the ballooning structures represent the short delaminations of the tegument. Eventually, hatched oncospheres shed the intermediate and peripheral layers which are attached to the basal layer of the tegument. Based on the above mentioned evidences, it is suggested that the huge vesicles are involved in the shedding of the distal layer of the capsular tegument. The ultrastructure of the tegument of the invaginated scolex resembles those described for adults as well as other cestode larvae. (Ruthman, 1963; Howell, 1965; Race et al, 1965; Morseth, 1967; Braton, 1968a, 1968b; Jha and Smyth, 1969; Rifkin et al, 1970; Baron, 1971; Cooper et al, 1975).

In the present study, subtegumentary cells, the cell bodies of the syncytial tegument, are ultrastructurally similar to type three cells of hatched oncospheres of H. citelli described by Collin (1968). However, Collin did not identify type three cells as the subtegumentary cells. Subtegumentary cells in the forebody of stage three larvae contain electron-dense granules which are not found in subtegumentary cells in the other regions. The presence of those granules correlate with the formation of microtriches suggesting that the electron-dense granules probably are precursors of electron-dense contents of microtriches. Subtegumentary cells in the capsular wall of late stage five larvae become vesiculated and have signs of degradation, but those in the invaginated scolex have no notable changes.

A hatched oncosphere of Hymenolepis citelli contains 29 muscle cells including 16 somatic muscle cells and 13 hook muscle cells (Collin 1969). Ogren (1972) demonstrated the exact anatomical pattern of the musculature in H. diminuta. A hatched oncosphere immediately begins metamorphosis. A hypothesis has been suggested that the metamorphosis is involved in the degeneration of the oncospherical musculature and the multiplication of the germinative cells (Slais, 1973). According to the hypothesis, muscle cells of stage two larvae differentiate from germinative cells instead of from pre-existing somatic or hook muscle cells. Several evidences of this report support this hypothesis. The hook muscles of stage two larvae are in the latter stage of the degradative processes. Thus, the degradative processes occur in the earlier stages (stage one larvae or hatched oncospheres). However, the fate of somatic muscles is unknown, but they probably

undergo the same degradative processes as hook muscles. In this study, the somatic muscles of stage two larvae resemble muscles of hatched oncospheres and adult tapeworms except for the absence of dense bodies. If the somatic muscles of stage two larvae are differentiated from pre-existing somatic muscles of hatched oncospheres, the dense bodies should be present in some or all of the somatic muscles of stage two larvae. Dense bodies are found in the muscles of hatched oncospheres (Collin, 1969), but are not found in the somatic muscles of stage two larvae. This suggests that the muscles of stage two larvae are not differentiated from pre-existing hook or somatic muscle cells; they are derived from germinative cells or primordial cells.

In this research, some cells in the middle of the forebody of stage three larvae are identified as muscle cells and are not found in other body divisions or in other stages of postembryonic development. They differ slightly from other muscle cells in the subtegumentary muscle layers. The ultrastructure of these cells suggests that they are relatively undifferentiated muscle cells of the prescolices.

The capsules of fully developed cysticercoids of Hymenolepis diminuta have been studied by Ubelaker et al (1970a) and Allison et al (1972). The ultrastructure of the fully developed capsules is well established, but the origin and differentiation of various layers of the capsule have been a topic of controversy for some time. This report, based on the observations of larval stages of the postembryonic development, has established some of the details of the origin and differentiation of the various layers of capsules.

The origin and differentiation of the capsular tegument and the subtegumentary muscle layer have been discussed previously. The ultrastructure of capsular muscles of H. diminuta is typical of cestode muscles as described by Lumsden and Byram (1968). The capsular muscle layer increases in length and thickness when postembryonic development proceeds and is probably the result of growth of pre-existing muscle cells.

Type five cells in the subtegumentary cellular layer of fully developed capsules are derived from type one cells, the primordial cells, in the midbody of stage three larvae. The type five cells in this report are equivalent to vesiculated cells in fully developed capsules of Hymenolepis diminuta described by Ubelaker et al (1970a). Based on the morphology, they suggested that fibrils and ground substance in the subtegumentary cellular layer, which is termed intermediate layer by them, are secretory products released by type five cells to the intercellular spaces. Several evidences of the present observations confirm Ubelaker's suggestion. First, the subtegumentary cellular layer in the developing capsules of stage three, four, and five larvae consists of muscle cells, subtegumentary cells and type five cells. The ultrastructure of both muscle cells and subtegumentary cells indicates that they are differentiated and specialized cells which perform certain functions. Apparently, they do not participate in the formation of fibrils and a ground substance. Second, the ultrastructure of type five cells resembles fibroblasts of mammalian connective tissues. Huge secretory vesicles of vesiculated cells described by Ubelaker et al (1970a) are not found in type five cells. However, several dilated cisternae of rough endoplasmic reticulum are in close

contact with cell membrane. Many membranous residuals are found in the intercellular ground substance. These findings suggest that membrane-bound visicles, presumably containing secretory substances, are released from type five cells to the intercellular spaces. The secretory substances probably contribute to the formation of fibrils and ground substance of the subtegumentary cellular layer and the loose fibrous layer.

The loose fibrous layer is not found in stage three larvae. It begins to form in young stage five larvae and increases in thickness as the development proceeds. The loose fibrous layer is located beneath the subtegumentary cellular layer. Apparently, type five cells are not like mammalian fibroblasts which are trapped in the fibrils and ground substances which are secreted by them. However, the exact mechanism of the assembling and distribution of fibrils and ground substance requires further investigation.

Allison et al (1972) suggested that the loose fibrous layer of Hymenolepis diminuta (which is termed fibrous zone by them) is formed by what they termed type A cells. Type A cells are located between the subtegumentary cellular layer and loose fibrous layer. The ultra-structure of type A cells resembles the oblique sections of fully developed flame cells or nephridial funnel cells in this report. The terminal organs of stage five larvae are also found between the subtegumentary cellular layer and loose fibrous layer. Furthermore, no cells which resemble the type A cells were found in the earlier developmental stages.

Numerous fine cytoplasmic processes are interspersed in the loose fibrous layer, but connections between these processes and their cell bodies were not found. Some of these processes, containing

microtubules, near the terminal organs of the protonephridial system probably are fine cytoplasmic processes of nephridial funnel cells, but the origin of the remaining processes is still unclear.

The fully developed dense fibrous layer consists of extremely long, attenuated, circular-arranged cytoplasmic processes of type six cells. Thus, the fibrous elements in the dense fibrous layer are really fine cytoplasmic processes. It is difficult to trace a given process from its origin to its end because of its length. The dense fibrous layer begins to form in the midbody of stage three larvae. Type six cells are derived from type one cells, the primordial cells, in the innermost layer of the subtegumentary cellular layer. New type six cells continue to form and add to the dense fibrous layer. The dense fibrous layer gradually increases in thickness as development proceeds. The type six cells in this report morphologically resemble the bipolar-shaped cells in the dense fibrous layer of Hymenolepis diminuta described by Allison et al (1972) and Voge (1960). Both Voge and Allison et al suggested that the bipolar-shaped cells are associated with fibrous elements formation in the dense fibrous layer.

Cooper et al (1975) indicated that the dense cellular layer of the cysticercoïd of H. diminuta is a reflexed neck tissue, formed during withdrawal of the prescolex of stage three larvae. Thus, the ultra-structure of the dense cellular layer resembles the scolex in general. The results of this study indicate that the dense cellular layer is not present in stage three larvae and is formed after a scolex is withdrawn into the central cavity. The cup-shaped dense cellular layer is connected to the posterior end of an invaginated scolex by a thin

stalk. Actually, the dense cellular layer is continuous with the invaginated scolex. These findings are in agreement with those of Cooper.

The ultrastructure of the terminal organs (flame cells) of the parasitic platyhelminthes has been described in detail by Welton (1969), Howells (1969), Gallagher and Threadgold (1967), Morseth (1967), and Bonsdorff and Telkka (1966). Wilson et al (1974) have reviewed the morphology and function of the protonephridial system. The ultrastructure of fully developed terminal organs in the present study in general resembles those described by the above mentioned investigators. Based on these reports and this study it indicates that the basic features of terminal organs are homologous throughout the parasitic platyhelminthes. Therefore, the morphology of terminal organs is well established. Unfortunately, there is no information available regarding the origin and differentiation of terminal organs. The present report describes the development of the terminal organs of Hymenolepis diminuta and it is hoped that this will establish a model applicable to other platyhelminthes.

Bugge (1902) cited by Wilson et al (Wilson et al, 1974) proposed that terminal organs are derived from three or four epithelial cells which are in turn derived from the lining of main protonephridial canal. The present observation demonstrates that the terminal organ is derived from two adjacent primordial cells of the subtegumentary cellular layer. Other cells adjacent to these two cells may be involved in the formation of a terminal duct but not in the formation of the terminal organ. However, the precise way of formation of the

interdigitation between these two cells is still unclear. Further studies are needed to reveal the interactions between these two types of cells.

The flame of the terminal organ of stage three larvae consists of about 17 loosely packed circular flagella and the central pairs of axial filaments in a given flame are not aligned in the same direction. The interdigitated area of the terminal organ of the stage three larvae is comprised of about eight flame cell rods and six nephridial funnel cell rods. The comparison of these features of stage three larvae with the fully developed terminal organ of stage five larvae indicates that the terminal organs of stage three larvae are relatively undifferentiated. It appears that further development of a terminal organ is involved in the formation of new flagella, flame cell rods, and nephridial funnel cell rods. It is understandable that new flagella add to the loosely packed flame, but it is difficult to interpret how these new rods connect to the tightly jointed interdigitated area.

Collecting ducts are first formed adjacent to terminal organs in stage three larvae. The origin of the cells, which contain the collecting ducts, is unclear. It seems reasonable to suggest that these cells are derived from type one cells. Wilson et al (1974) reported that the collecting duct walls are syncytial in adult Hymenolepis. No junctions were observed between collection duct cells. Presumably, the collecting duct walls of its cysticeroid are also syncytial.

Occasionally, two collecting ducts are found in a single cell. This suggests that the collecting ducts are the result of the coalescence of many smaller vesicles which are present in the developing cells.

The lumens of collecting ducts increase in diameter and form bead-like cytoplasmic processes as the development proceeds. Thus, a fully developed collecting duct is surrounded by a thin rim of cytoplasm. The nuclei of fully developed collecting duct cells are spindle shaped and displaced to a corner of the cell.

Flame cells, nephridial funnel cells and collecting duct cells begin to differentiate simultaneously in the subtegumentary cellular layer of stage three larvae. In addition, the interactions between flame cells and nephridial funnel cells, as mentioned previously, suggest a considerable degree of communication and mutual influence among these cells.

The formation of calcareous corpuscles of parasitic platyhelminthes has been studied in detail by Nieland and Brand (1969), Martin and Bils (1964), Chowdhury et al (1961), and Brond et al (1960). All of these reports are based on the observations from adult worms. The corpuscle formation of cysticercoïds in this report is similar to those of adult cestodes (Nieland and Brand, 1969; Chowdhury et al, 1961; and Brand et al, 1960). This study also indicates that in the cyclophyllid tapeworms the formation of corpuscles is fairly uniform. This study also indicates that the formation of calcareous corpuscles in larval cestodes differs from that of trematodes confirming the work of Martin and Bils, 1964. They demonstrated that the corpuscles are formed in main collecting vessels of the protonephridial system of trematode metacercariae. However, the corpuscles of the cysticercoïds in the present report are formed inside the cells. All of the above mentioned authors have suggested that the corpuscle formation occurs in

the mesenchymal or parenchymal cells which are undifferentiated cells. In this work calcareous corpuscles were not observed until stage three larvae. While it is not possible to ascertain with certainty, it seems probable that they are formed in type one cells.

SUMMARY

The ultrastructures of larval stages two through five of the postembryonic development of the rat tapeworm, Hymenolepis diminuta, were studied. The interactions of host haemocytes and postembryonic larval stages were described.

The ovoid-shaped stage two larva has a central cavity which is surrounded by a tegument and a subtegumentary cellular layer. The syncytial tegument is connected to subtegumentary cells by cytoplasmic extensions, and its free surface bears numerous microvilli. The subtegumentary cellular layer consists of type one cells (primordial cells), subtegumentary cells, and muscle cells. The cellular morphology of these cells was described and the origin of these cells was suggested. The ultrastructure of larval hooks and hook muscles, which attach on the posterior end of stage two larvae was also described.

The stage three larva consists of a forebody, a midbody, and a hindbody. The forebody begins to differentiate into a scolex which consists mainly of primordial and muscle cells. Cytoplasmic extensions (microtriches) start to form on the free surface of the tegument of the scolex. The midbody has a central cavity which is surrounded by a capsule with outer and inner layers. The outer layer is comprised of primordial and type five cells. Some primordial cells of the outer layer differentiate into the protonephridial system. The inner layer is comprised of cell types four and six. Calcareous corpuscle

formation cells are also found in the inner layer of the capsule. The round, solid hindbody consists of cell types one, two, and six. The fine structure of cell types four, five, and six was described and the origin of these cells was discussed.

The stage four and stage five larvae consist of invaginated scolices which are surrounded by capsules. The tegument of an invaginated scolex bears microtriches which resemble those of adult Hymenolepis and other adult tapeworms. The scolex has four well developed suckers. In addition to muscle cells, the scolex consists principally of primordial cells. The outer layer of the capsule consists of a subtegumentary cellular layer and a loose fibrous layer. The subtegumentary cellular layer is comprised mainly of type five cells, and the loose fibrous layer is comprised of numerous densely-packed fibers. A well developed protonephridial system is found in the area between the subtegumentary cellular layer and the loose fibrous layer. The inner layer of the capsule consists of a dense fibrous layer and a dense cellular layer. The dense fibrous layer consists of type six cells and their extremely long, attenuated, circularly arranged cytoplasmic processes. The dense cellular layer of the inner layer of the capsule represents reflexed neck tissue, formed during withdrawal of the scolices of stage three larvae. Thus, in general, the ultrastructure of this layer resembles the scolex. Histogenesis of these layers of the capsule was discussed.

APPENDIX I

FIGURES

Figure 1

Light photomicrograph (LPM) of a section through a stage two larva; the arrow points to the anterior end.

bh: beetle haemocyte

cc: central cavity X 430

Figure 2

LPM of a high-power view of the anterior end of a stage two larva.

bb: brush border

bh: beetle haemocyte

cc: central cavity

T₁: type one cell

T₂: type two cell

T₃: type three cell

tg: tegument X 1,630

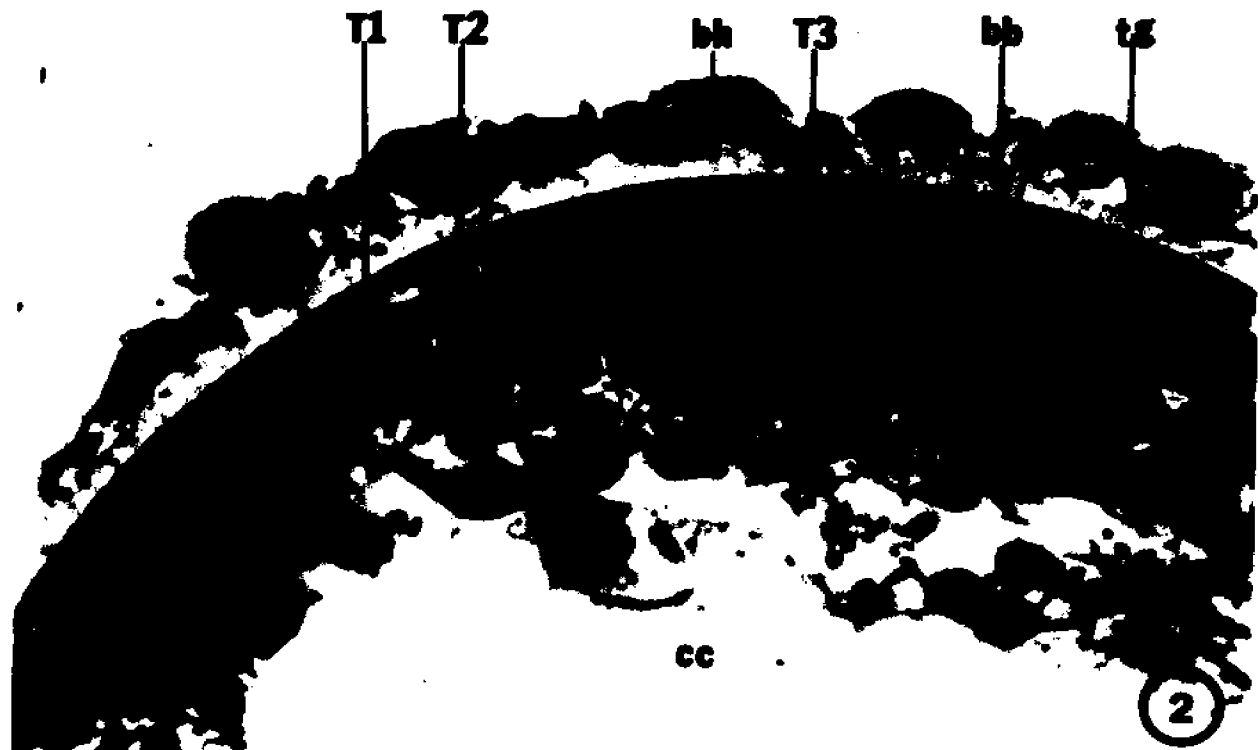
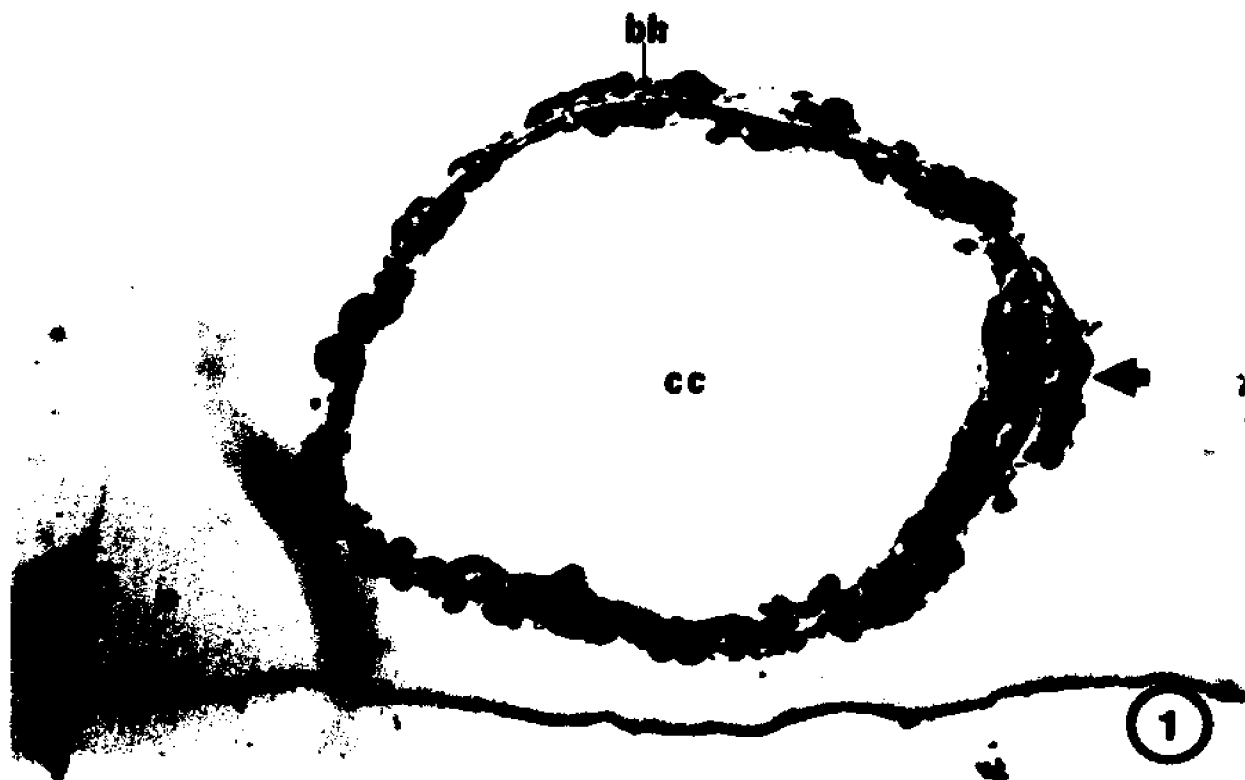


Figure 3

LPM of a section through a stage two larva showing the distribution of cell types one, two, and three.

bh: beetle haemocyte

cc: central cavity

T_{1s}: small type one cell

T_{1l}: large type one cell

T₂: type two cell

T₃: type three cell

X 675

Figure 4

LPM of a high-power view of a type three cell.

bh: beetle haemocyte

cc: central cavity

T₃: type three cell

X 1,630



Figure 5

LPM of a cross section through the forebody of a stage three larva; the arrows point to the rudimentary suckers. X 675

Figure 6

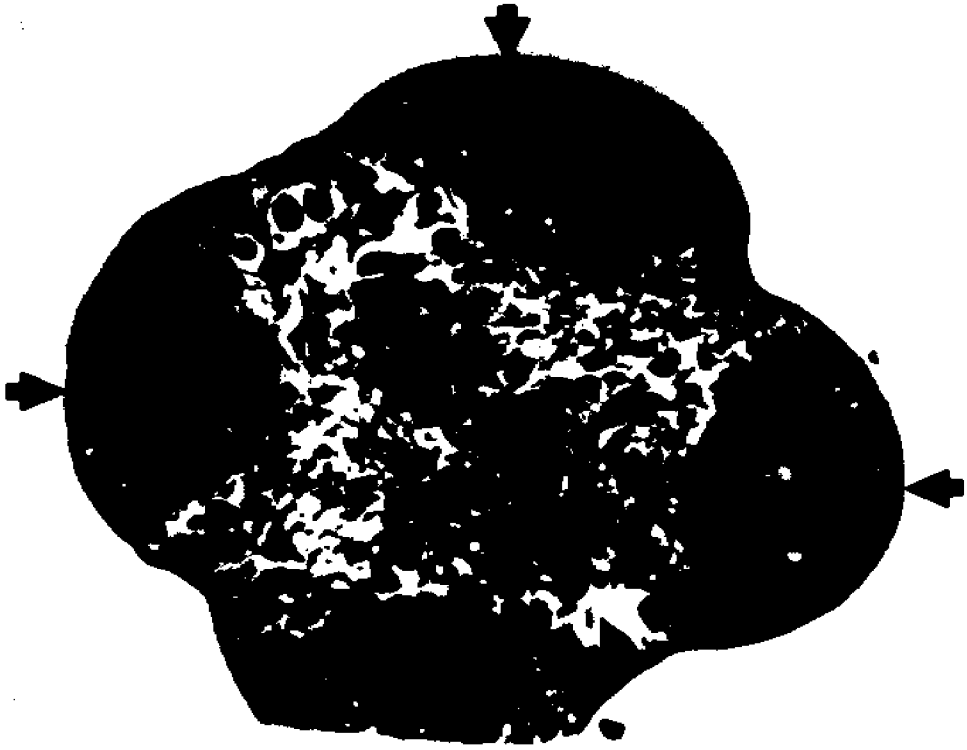
LPM of a high-power view of the rudimentary sucker of a stage three larva. The arrow points to the inner border of a rudimentary sucker.

T₁: type one cell

T₂: type two cell

T₃: type three cell

X 1,630



5



6

Figure 7

LPM of a high-power view of a type four cell of a rudimentary sucker.

T₂: type two cell

T₃: type three cell

T₄: type four cell X 1,630

Figure 8

LPM of a cross section of the transitional zone between the forebody and modbody of a stage three larva.

T₃: type three cell

T₄: type four cell X 675

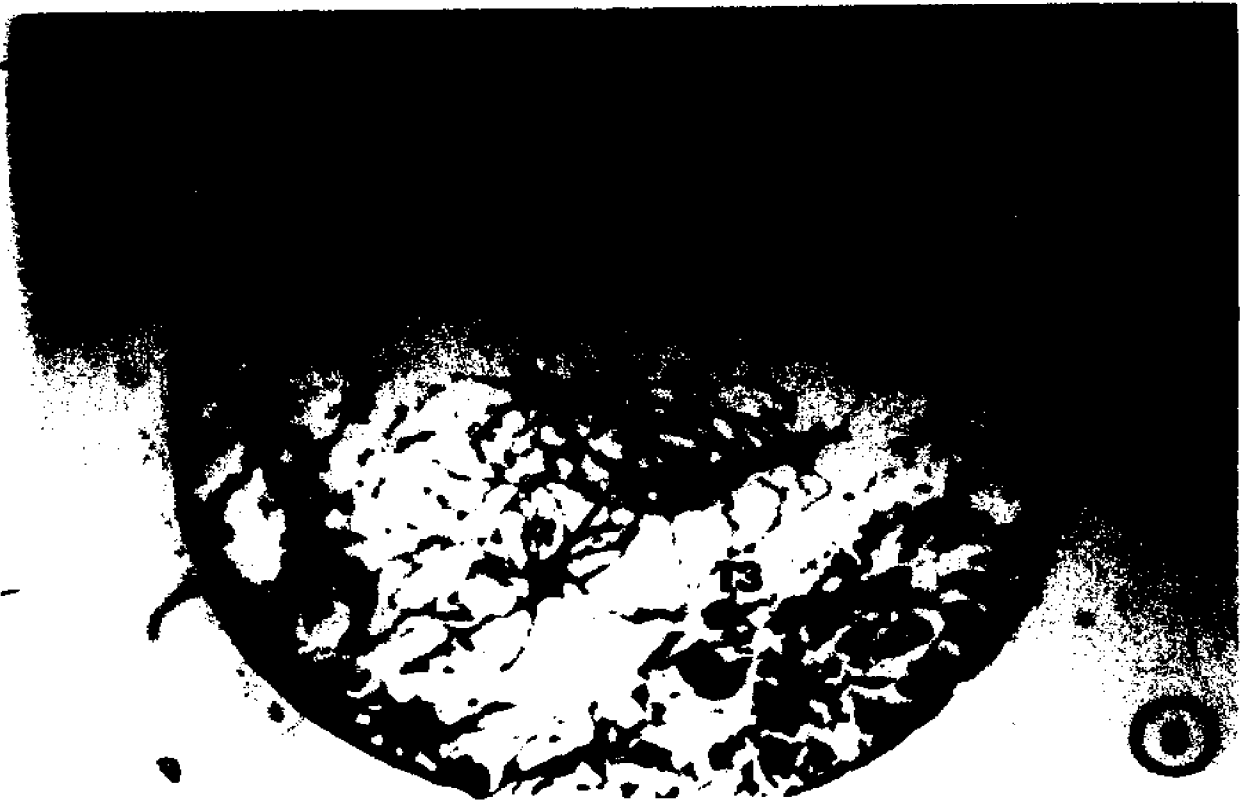


Figure 9

LPM of a high-power view of the transitional zone of a stage three larva. The arrow points to a cluster of type three cells.

X 1,630

Figure 10

LPM of a high-power view of the loose network in the middle of the transitional zone of a stage three larva. The arrow points to a type four cell and some of its highly branched cytoplasmic processes.

X 1,630

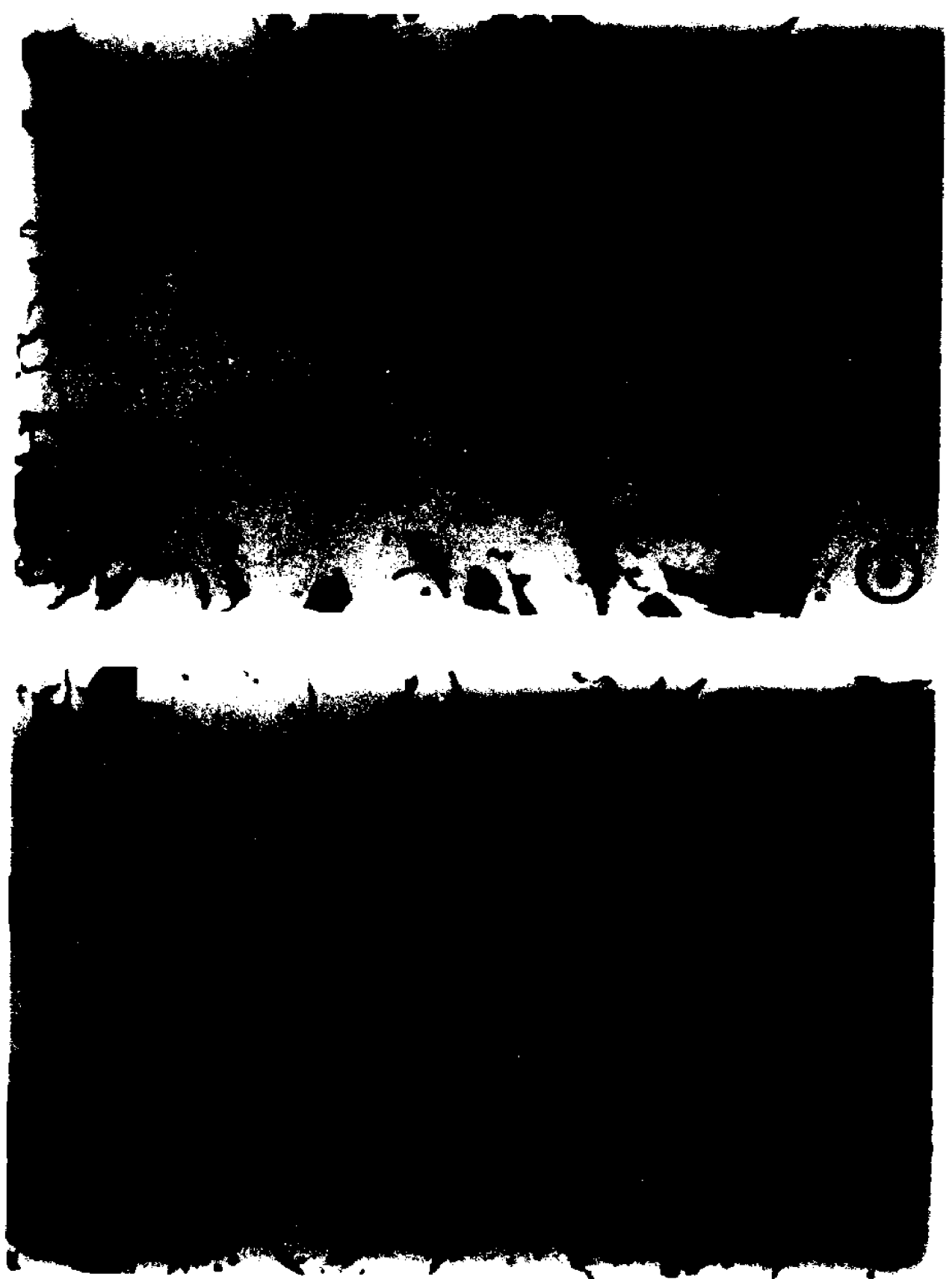


Figure 11

LPM of a high-power view of the transitional zone of a stage three larva. The arrows point to cells forming calcareous corpuscles.

X 1, 630

Figure 12

LPM of a cross section through the midbody of a stage three larva.

cc: central cavity

cl: cellular layer

ifl: inner fibrous layer

ofl: outer fibrous layer

T₂: type two cell

T₄: type four cell

T₅: type five cell

X 675



Figure 13

LPM of a high-power view of the subtegumentary cellular layer of the midbody of a stage three larva. The arrows point to various stages of differentiation of large type one cells.

T₂: type two cell

T₅: type five cell X 1,630

Figure 14

LPM of a high-power view of the outer and inner fibrous layers of the midbody of a stage three larva.

T₆: type six cell

ifl: inner fibrous layer

ofl: outer fibrous layer X 1,630



Figure 15

LPM of a cross section through the hindbody of a stage three larva. The solid arrow points to the subtegumentary cellular layer and the open arrow points to the core.

T₆: type six cell

X 675

Figure 16

LPM of a high-power view of the subtegumentary cellular layer of the hindbody of a stage three larva.

T₁: type one cell

T₂: type two cell

T₅: type five cell

X 1,630



T5 T6



Figure 17

LPM of a high-power view of the core of the hindbody of a stage three larva.

T₁: type one cell X 1,630

Figure 18

LPM of a cross section through the anterior end of a stage five larva with the opening of the anterior canal.

ac: anterior canal

T₂: type two cell

T₅: type five cell X 675



Figure 19

LPM of a cross section through the middle portion of the anterior canal of the stage five larva.

ac: anterior canal

T₂: type two cell

T₅: type five cell X 430

Figure 20

LPM of a cross section through the end of anterior canal of a stage five larva. The arrow points to the plug.

ac: anterior canal

T₂: type two cell

T₅: type five cell

T₆: type six cell X 430



Figure 21

LPM of a cross section through the plug of a stage five larva. The arrow points to the plug. X 430

Figure 22

LPM of a cross section through the invaginated scolex of a stage five larva.

sc: scolex

X 430



21



Figure 23

LPM of a high-power view of the invaginated scolex of a stage five larva. The solid arrow points to the muscle and the open arrow points to the inner border of a well developed sucker.

X 1,630

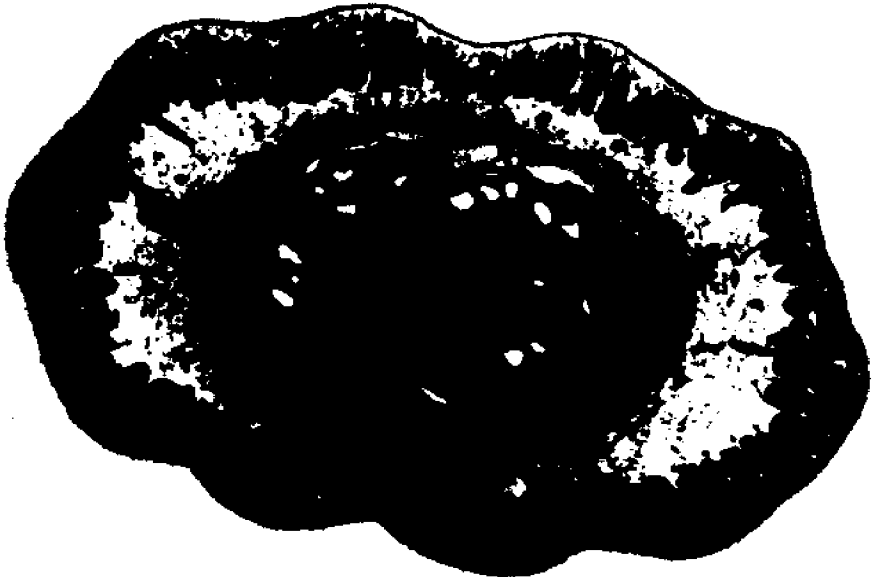
Figure 24

LPM of a cross section through the anterior end of the invaginated scolex of a stage five larva. The holes, which are indicated by arrows, represent calcareous corpuscles which have been removed during sectioning.

X 430



23



24

Figure 25

LPM of a high-power view of a stage five larval capsule.

df1: dense fibrous layer

dscl: densely stained cellular layer

im: intermediate layer

lfl: loose fibrous layer

T₅: type five cell

T₆: type six cell X 1,630

Figure 26

LPM of a high-power view of both loose and dense fibrous layers of a stage five larval capsule.

df1: dense fibrous layer

dscl: densely stained cellular layer

lfl: loose fibrous layer

T₆: type six cell X 1,630



Figure 27

LPM of a cross section through the tail of a stage five larva.

T_3 : type three cell X 675

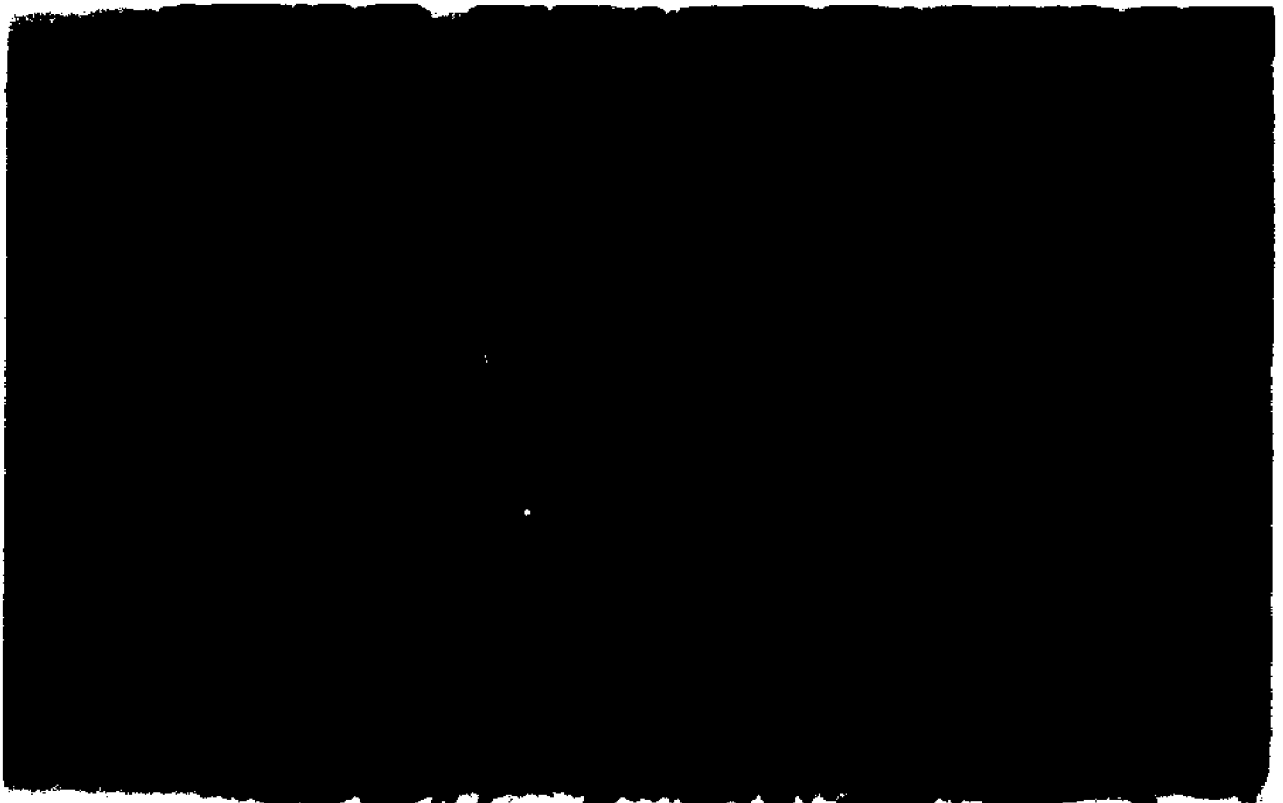
Figure 28

LPM of a high-power view of the tail of a stage five larva.

T_1 : type one cell

T_2 : type two cell

T_4 : type five cell X 1,630



Figures 29 to 43 are electron photomicrographs of stage two larvae.

Figure 29

A high-power view of a beetle haemocyte with phagocytic vacuoles and extremely long, branched microvilli. The arrow indicated dilated vesicles at the tips of microvilli.

BH: beetle haemocyte

PV: phagocytic vacuole

S2: stage two larva

V: microvilli

X 31,200



Figure 30

A layer of beetle haemocytes attached to a stage two larva.

BH: beetle haemocyte

S2: stage two larva

V: microvilli

X 8,350

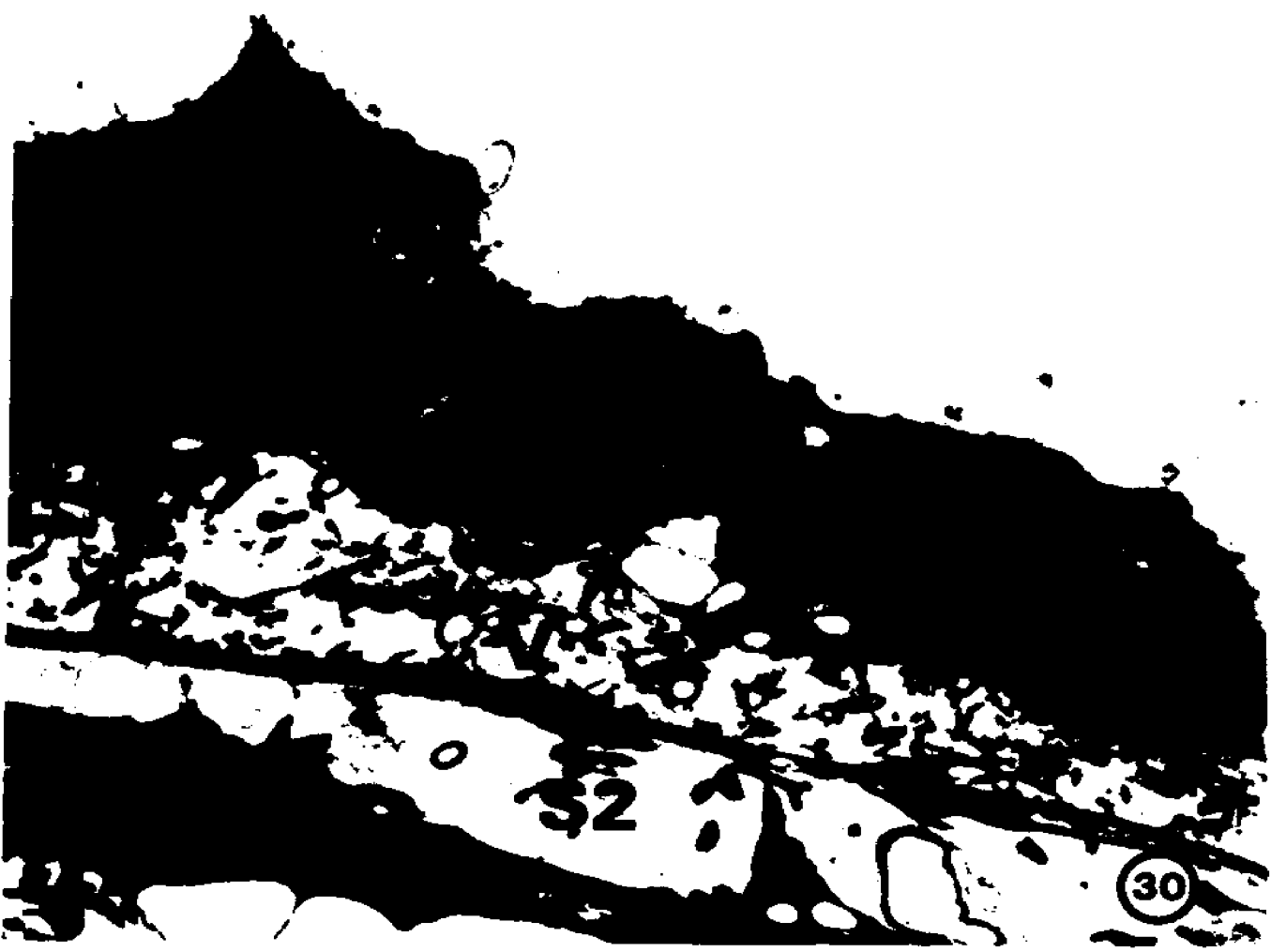


Figure 31

High-power view of an active beetle haemocyte which is attached to a stage two larva.

ER: endoplasmic reticulum

L: secondary lysosome

M: mitochondria

N: nucleus

NS: nucleolus

X 31,200

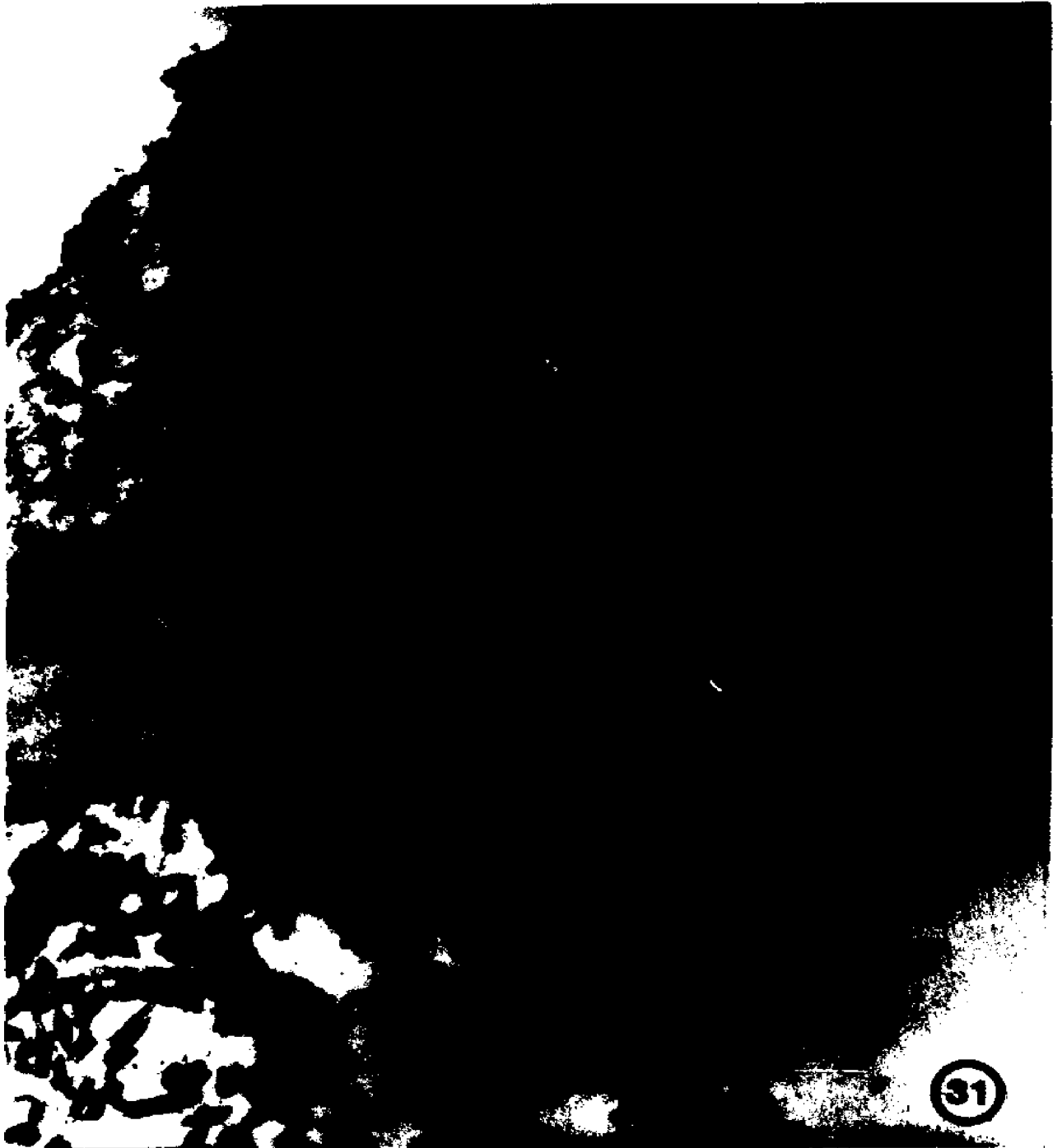


Figure 32

A beetle haemocyte, which attaches to a late stage two larva, undergoes degradative changes.

L: secondary lysosome

LD: lipid droplet

N: nucleus

PLV: phago-lysosomal vacuole

S2: stage two larva

V: microvilli

X 8,350



Figure 33

High-power view of a cytolyzed beetle haemocyte with a pyknotic nucleus.

N: nucleus

S2: stage two larva

V: microvilli X 16,970

Figure 34

Low-power view of an un-nucleated syncytial tegument, and its nucleated cell bodies, the subtegumentary cells. An arrow indicates many tenuous cytoplasmic processes which connect the tegument to subtegumentary cell.

ST: subtegumentary cell

T: tegument X 4,900

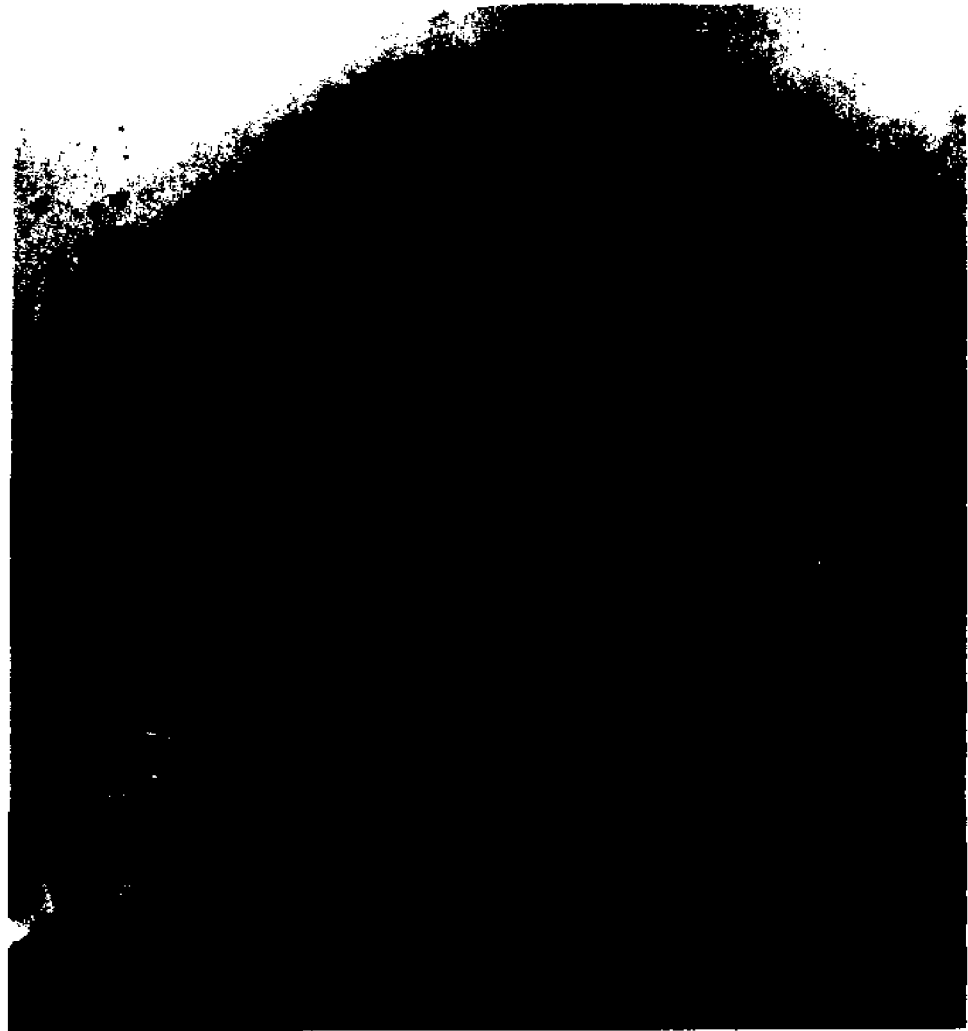


Figure 35

A subtegumentary cell and tegument of a stage two larva.

GL: glycogen granules

M: mitochondria

MG: melanin-like granules

MS: muscle

N: nucleus

NS: nucleolus

T: tegument

V: microvilli

VC: vesicle

X 14,700



Figure 36

High-power view of a muscle cell of a stage two larva

ER: endoplasmic reticulum

M: mitochondria

N: nucleus

ST: subtegumentary cell

T: tegument X 16,970

Figure 37

High-power view of a cytoplasmic process of a muscle cell of a stage two larva. An arrow indicates myofilaments.

MS: muscle

ST: subtegumentary cell X 16,970



Figure 38

The subtegumentary cellular layer of a stage two larva consists of various cell types. An arrow indicates thin cytoplasmic processes which separate the subtegumentary cellular layer from the central cavity.

C: central cavity

ST: subtegumentary cell

T₁: type one cell

X 9,000

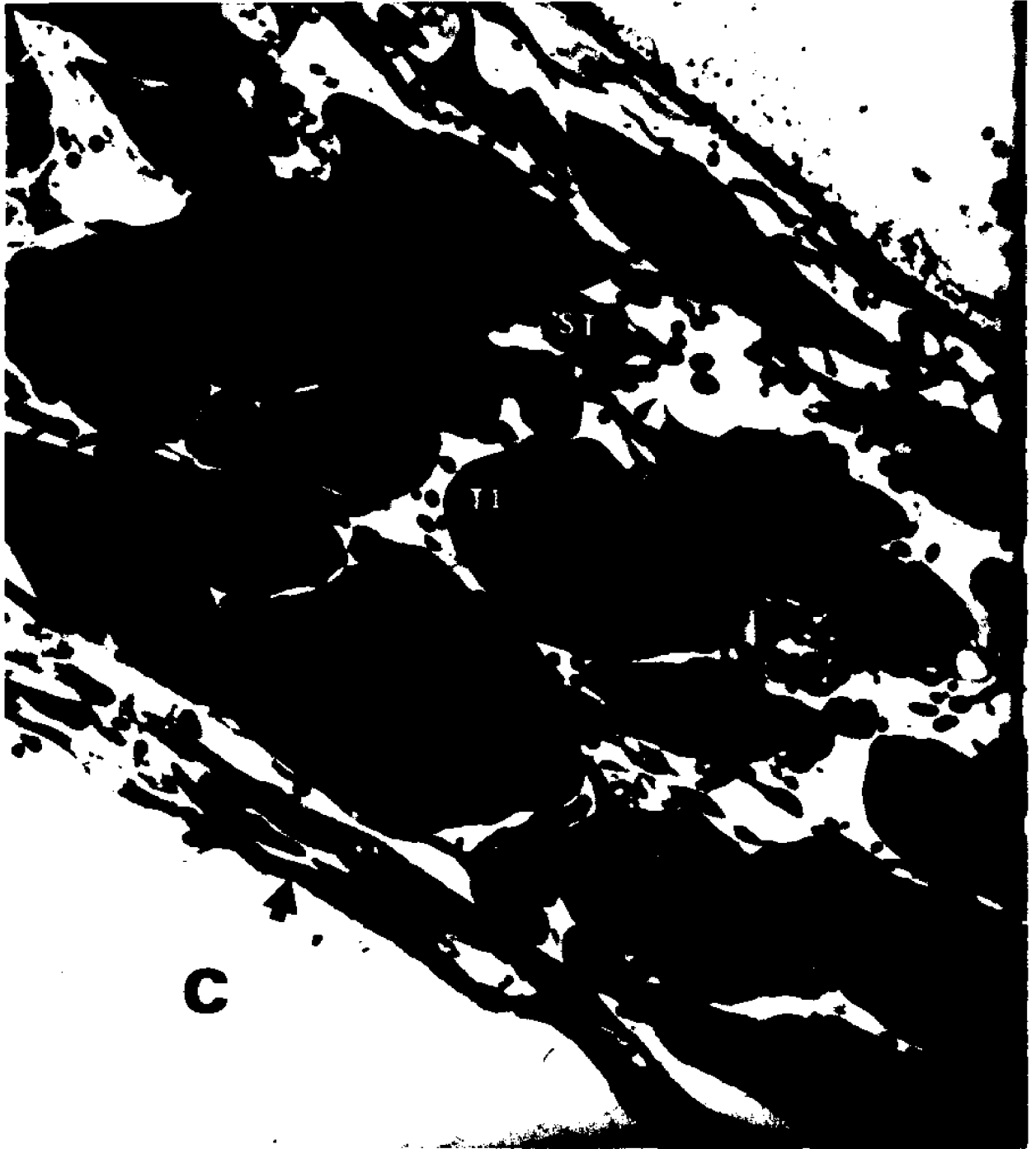


Figure 39

High-power view of type one cells.

ER: endoplasmic reticulum

M: mitochondria

N: nucleus

NS: nucleolus

X 20,880



Figure 40

An oblique section of a larval hook.

BL: blade

GA: guard

H: handle

MS: muscle

X 7,200

Figure 41

High-power view of the basal region of a larval hook. Arrows indicate the cup-shaped socket.

HO: hook

MS: muscle

X 16,970

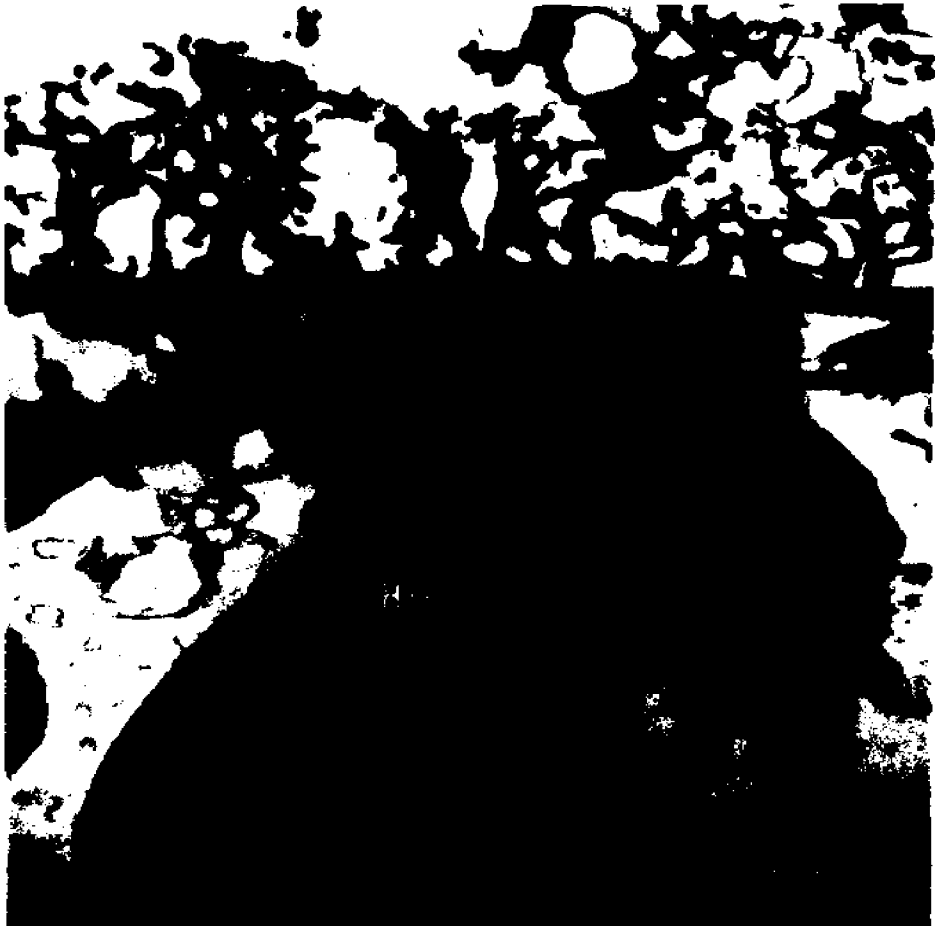
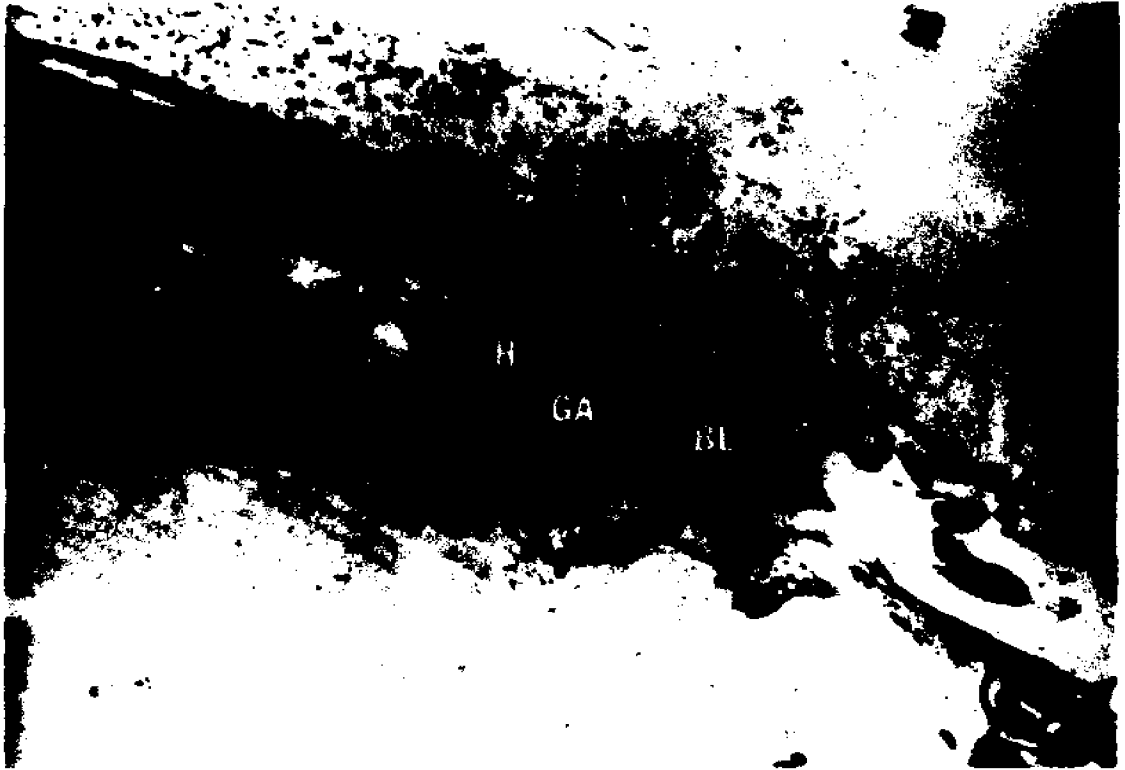


Figure 42

High-power view of a decomposed area of a larval hook muscle. An arrow indicates the decomposed area.

HO: hook

MS: muscle

ST: subtegumentary cell X 20,880



Figure 43

High-power view of an oblique section of a larval hook.

CO: core

MF: middle fibrous layer

MS: muscle

O: opaque outer granular layer X 32,000



Figures 44 to 64 are electron photomicrographs of stage three larvae.

Figure 44

The tegument and muscles of the forebody of a stage three larva. The free surface of the tegument consists of numerous microvilli and a few microtriches.

MS: muscle

MT: microtriche

T: tegument

V: microvilli

X 14,700

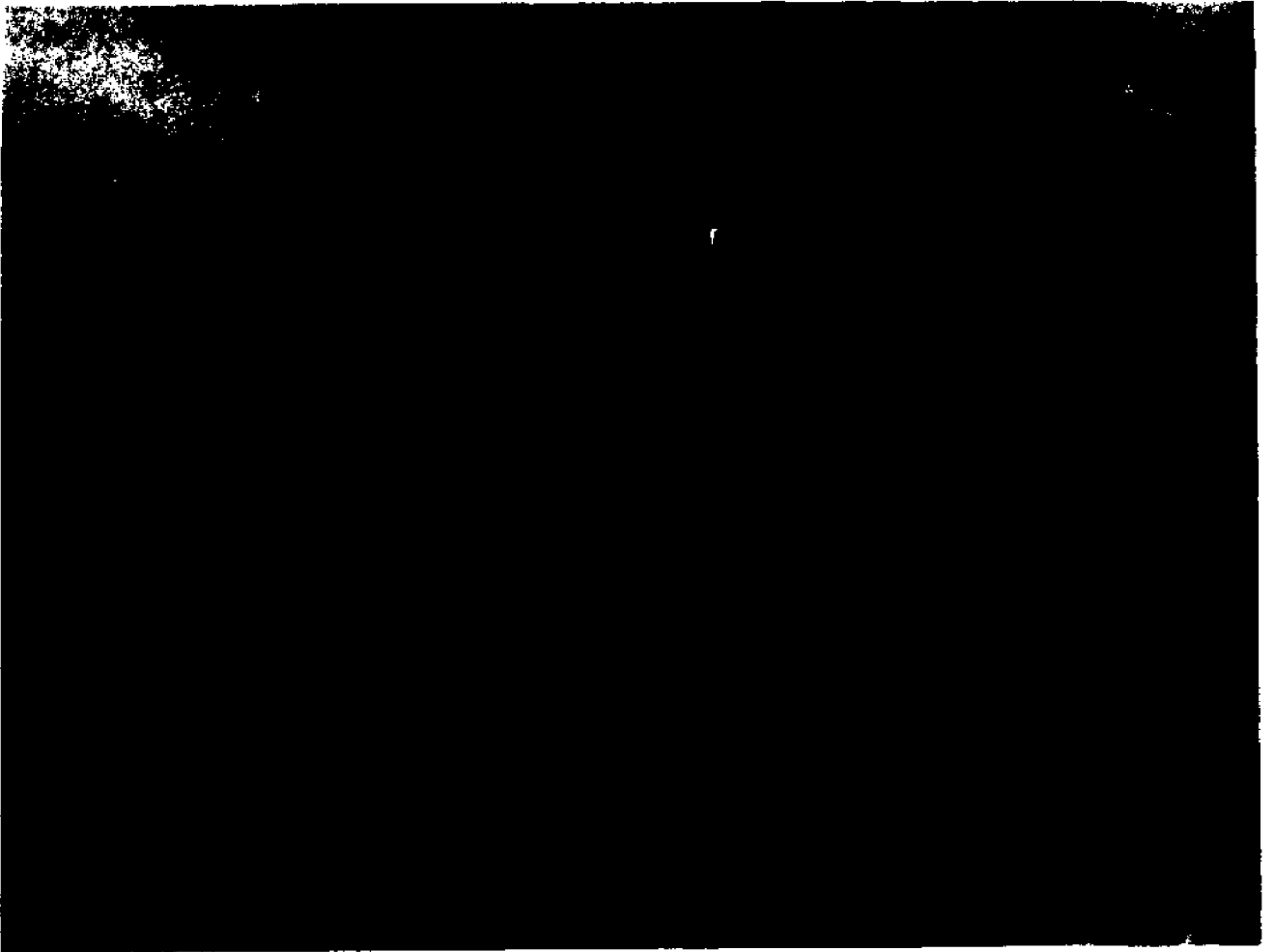


Figure 45

The tegument of the forebody of a stage three larva showing a tegumentary invagination. Arrows indicate the tegumentary invaginations.

MS: muscle

T: tegument

X 12,800

Figure 46

High-power view of dense bodies occur among myofilaments. Arrows point to dense bodies.

X 46,800



Figure 47

High-power view of the medullary region of the forebody of a stage three larva with a variety of cell types. An arrow indicates a binucleated subtegumentary cell.

MS: muscle

ST: subtegumentary cell

T: tegument

T₁: type one cell

X 16,970

Figure 48

The medullary region of the forebody of a stage three larva showing a cluster of muscle cells.

MS: muscle

X 7,200

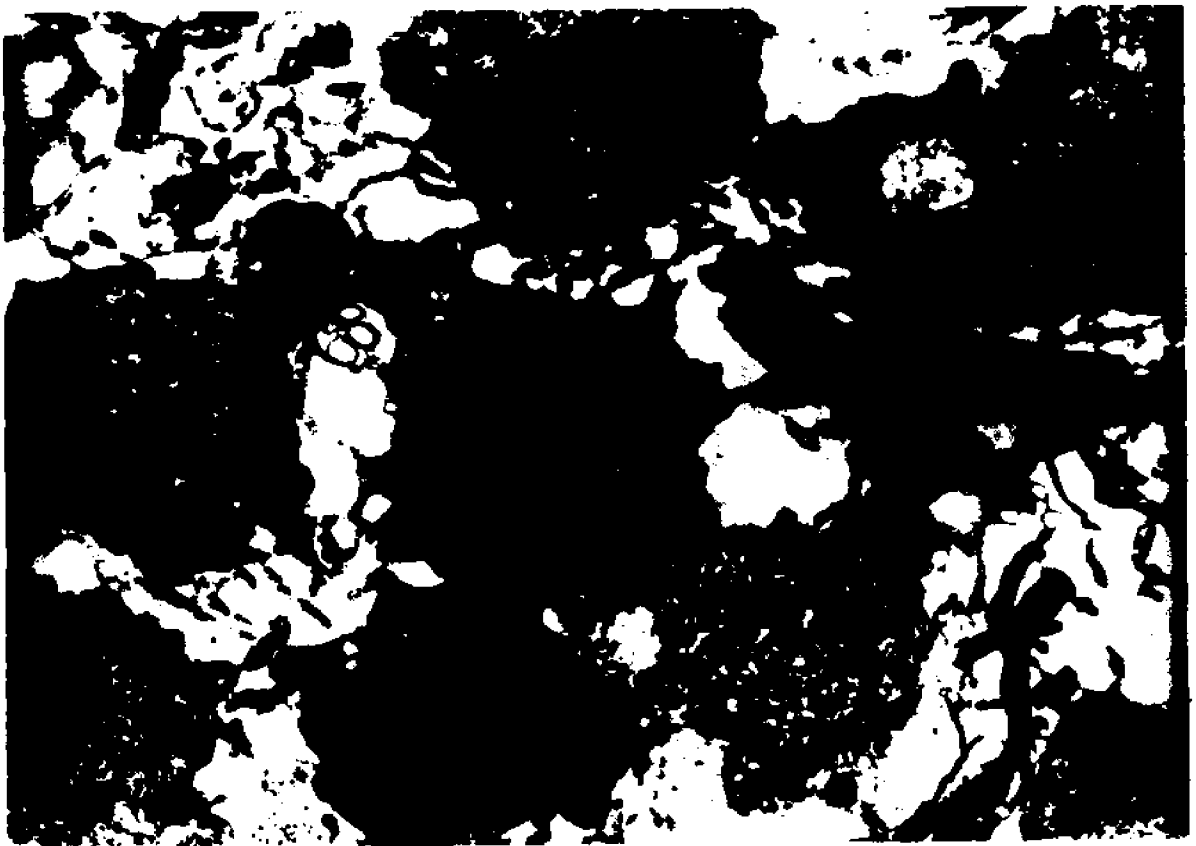


Figure 49

The transitional zone of a stage three larva with a developing terminal organ of a protonephridial system.

F: flame

FC: flame cell

FR: flame cell rod

NC: nephridial funnel cell

NR: nephridial funnel cell rod X 7,200

Figure 50

High-power view of a cross section through the interdigitated region of a terminal organ of a protonephridial system of a stage three larva. Arrows indicate leptotriches of flame cell rods.

F: flame

FC: flame cell

FR: flame cell rod

NC: nephridial funnel cell

NR: nephridial funnel cell rod X 24,750



Figure 51

High-power view of an oblique section through a terminal organ of a stage three larva showing a desmosome-like structure joining a flame cell rod to a nephridial funnel cell rod.

F: flame

FC: flame cell

FR: flame cell rod

NC: nephridial funnel cell

NR: nephridial funnel cell rod X 16,970

Figure 52

A longitudinal section of a terminal organ of a stage three larva.

F: flame

FC: flame cell

FR: flame cell rod

MS: muscle

NC: nephridial cell

NR: nephridial cell rod

T₁: type one cell X 8,350

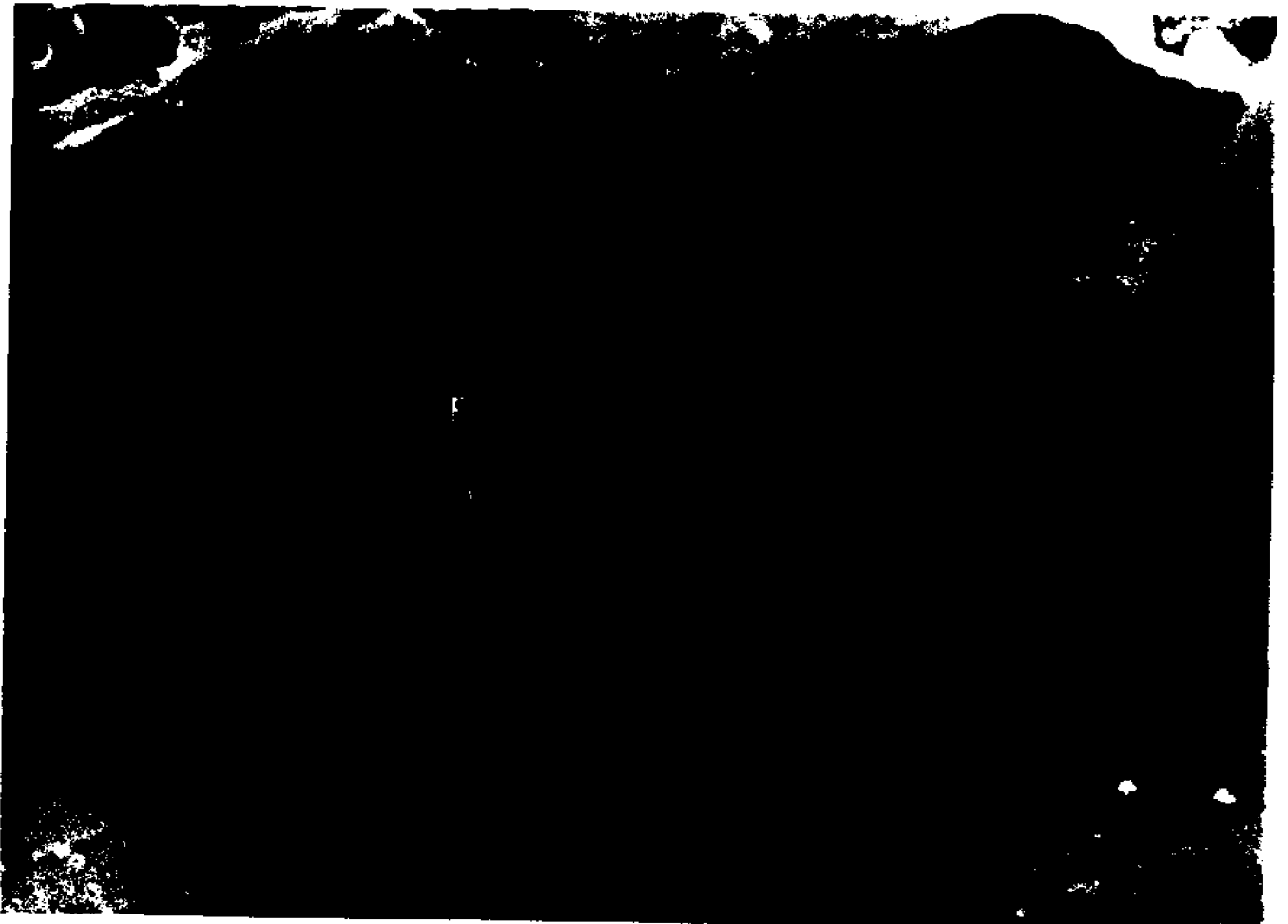
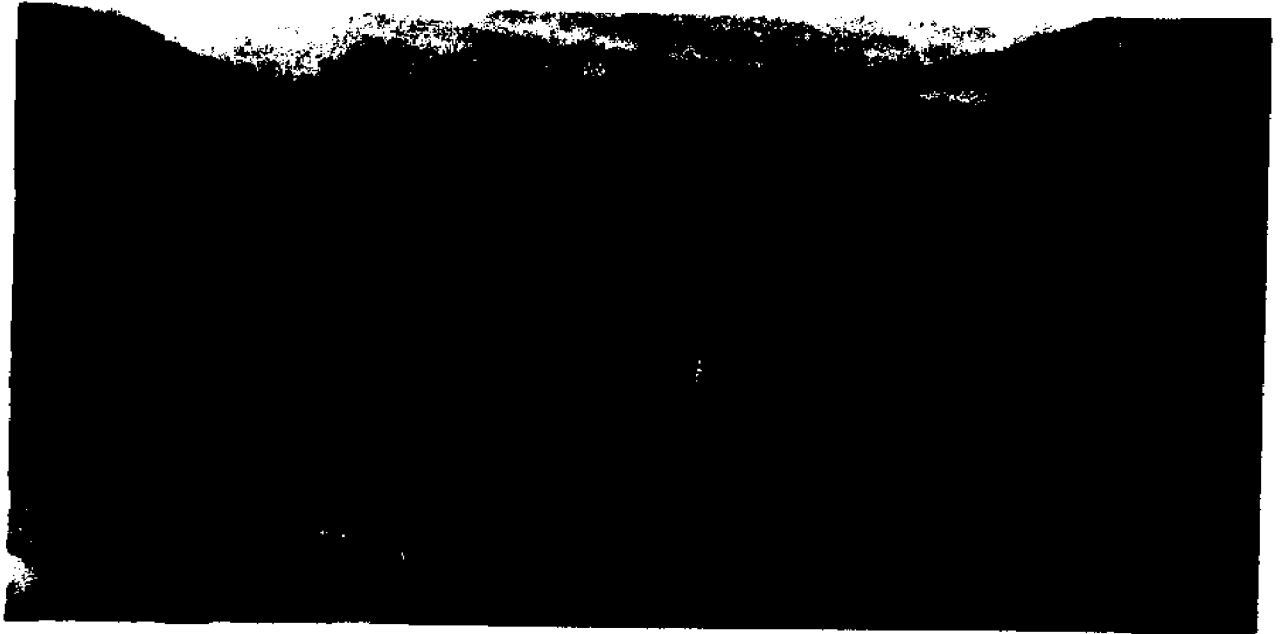


Figure 53

High-power view of a developing collecting duct cell of a stage three larva. Arrows indicate cytoplasmic processes.

CD: collecting duct

MS: muscle

NS: nucleolus

VC: vesicle

X 20,880



Figure 54

Type four cells and their cytoplasmic processes. Arrows point to cytoplasmic processes filled with beta glycogen granules.

X 6,800



Figure 55

High-power view of a type four cell and its cytoplasmic processes.

ER: endoplasmic reticulum

M: mitochondria

N: nucleus

NS: nucleolus

X 15,600

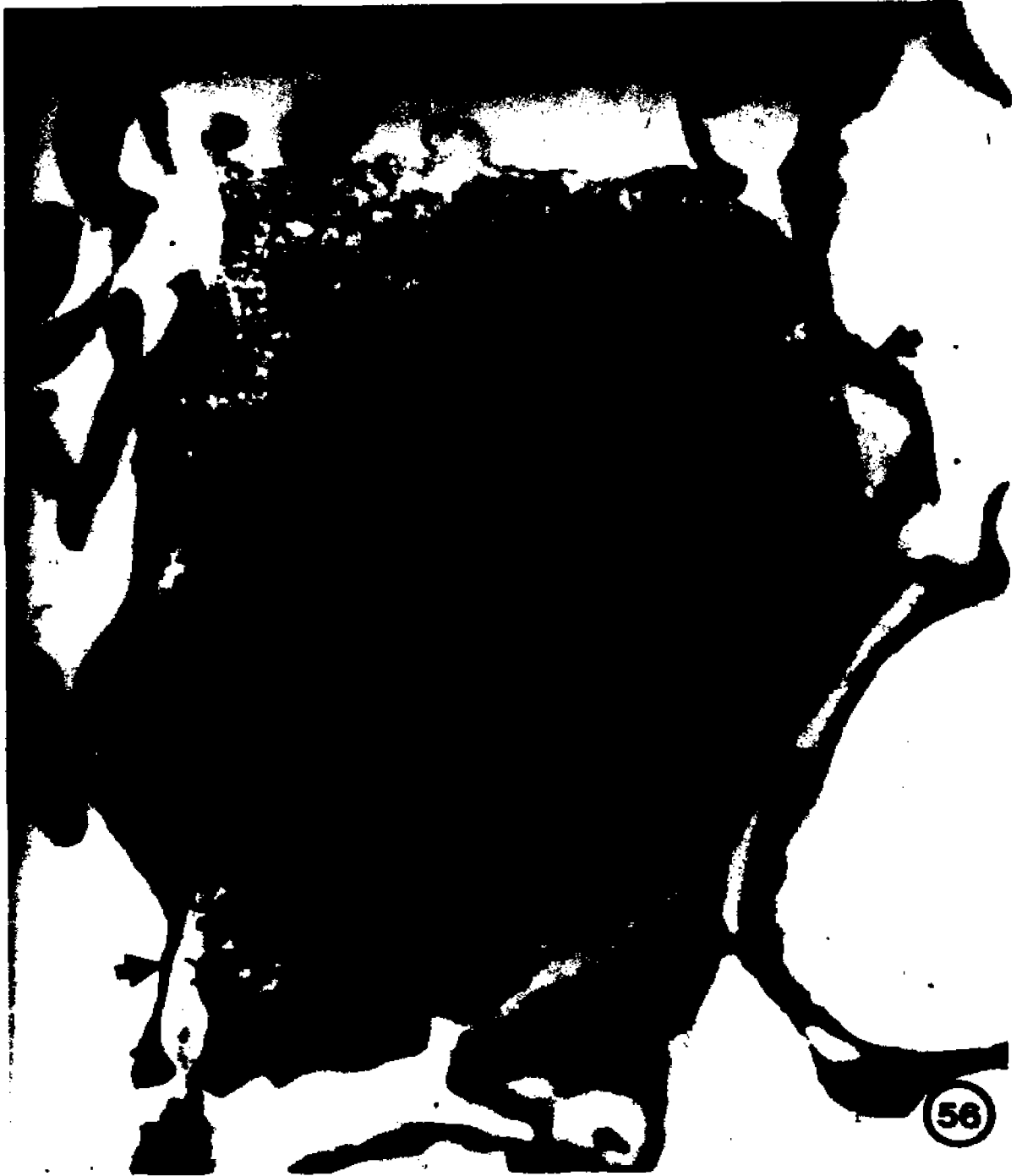


Figure 56

Cytoplasmic processes of type four cells are in contact with a muscle cell. Arrows indicate cytoplasmic processes which are in contact with the muscle cell.

MS: muscle

X 15,600



58

Figure 57

A calcareous corpuscle formation cell is surrounded by cytoplasmic processes of type four cells. Arrows indicate cytoplasmic processes of type four cells.

CC: calcareous corpuscle

T₄: type four cell

X 9,000



Figure 58

A calcareous corpuscle formation cell. Arrows indicate vermiform cytoplasmic folds.

CC: calcareous corpuscle

DC: dense center of a calcareous corpuscle

X 15,600



Figure 59

A young calcareous corpuscle formation cell consists of a less-dense matrix.

CC: calcareous corpuscle

DC: dense center of a calcareous corpuscle

X 16,970

Figure 60

High-power view of a muscle cell of a stage three larva.

M: mitochondria

N: nucleus

NS: nucleolus

RC: dilated cisternae

X 16,970



Figure 61

High-power view of type five cells of a stage three larva.

ER: endoplasmic reticulum

M: mitochondria

N: nucleus

NS: nucleolus

RC: dilated cisternae

T₅: type five cell

X 14,700

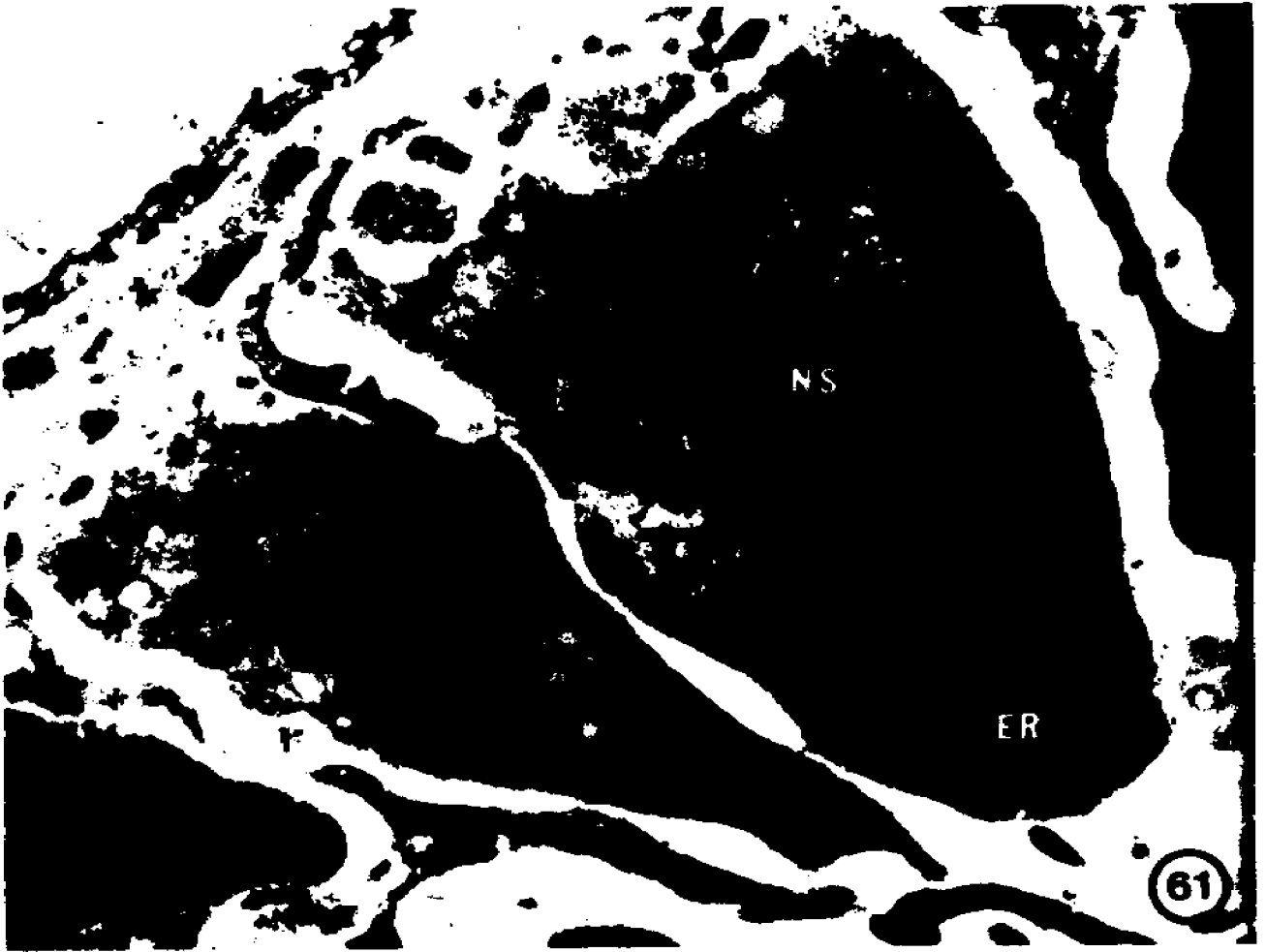


Figure 62

Low-power view of the midbody of a stage three larva showing various cell types.

LD: lipid droplet

MS: muscle

ST: subtegumentary cell

T₁: type one cell

T₅: type five cell

T₆: type six cell

X 9,000



Figure 63

The outer fibrous layer of a stage three larva having type six cells and their fibrous elements.

LD: lipid droplet

FE: fibrous elements

M: mitochondria

T₆: type six cell

X 9,000



Figure 64

High-power view of a type four cell and its highly branched cytoplasmic processes of the inner fibrous layer.

X 9,000



Figures 65 to 83 are electron photomicrographs of stage five larvae.

Figure 65

The tegument and its cell body, a subtegumentary cell of a stage five larva. Arrows indicate large vesicles containing irregularly shaped, electron-opaque cores.

DL: distal layer

MS: muscle

PL: proximal layer

ST: subtegumentary cell

T: tegument

X 15,600



Figure 66

The tegument and subtegumentary cellular layer of a stage five larva.
An arrow indicates the tegumentary surface swelling.

T: tegument

T₅: type five cell

ST: subtegumentary cell X 8,350

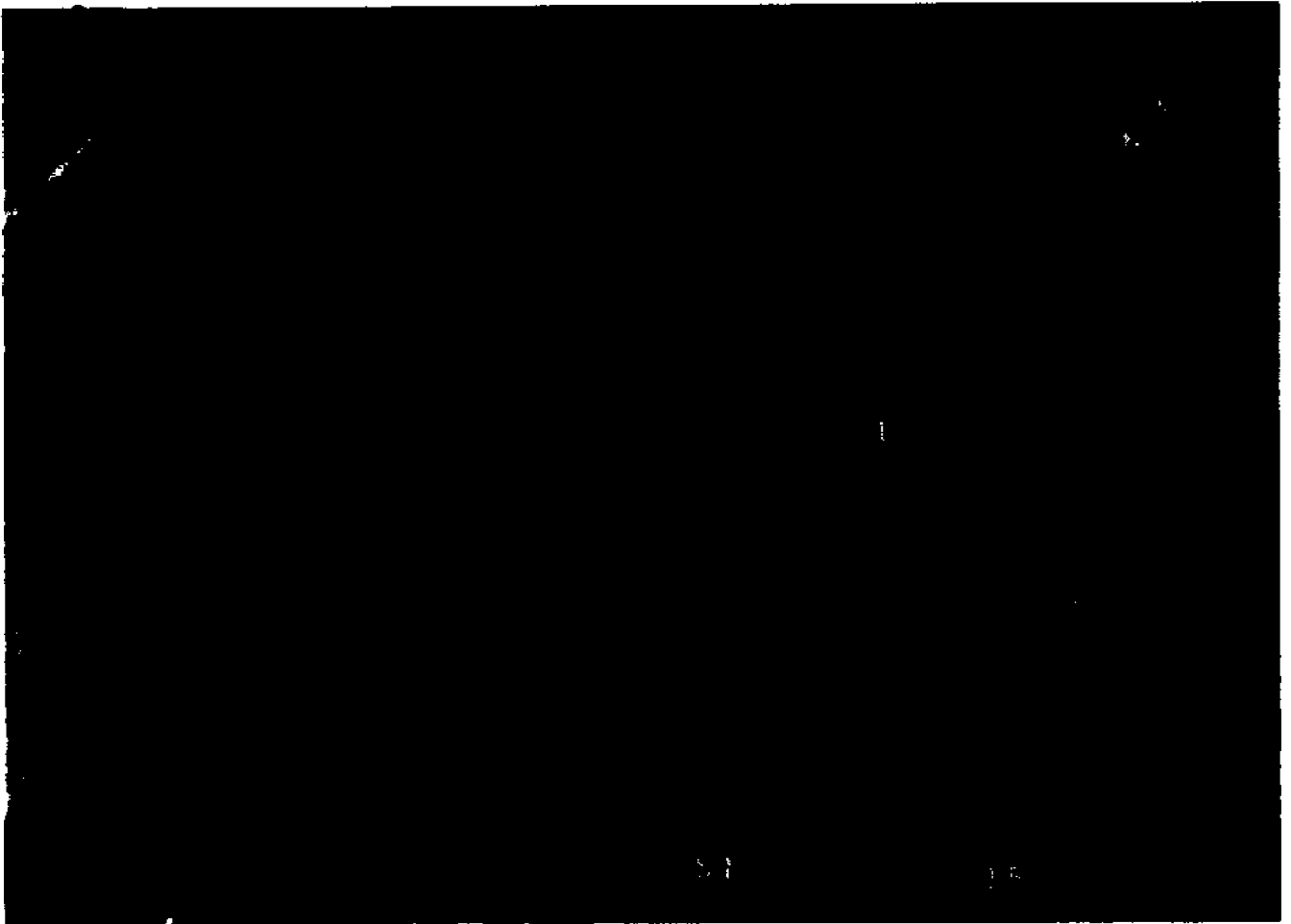


Figure 67

The tegument and subtegumentary cellular layer of a stage five larva having type five cells and a vesiculated subtegumentary cell.

ST: subtegumentary cell

T: tegument

T₅: type five cell

X 8,350



Figure 68

The tegument and subtegumentary cellular layer of a stage five larva having type five cells with elongated distal ends. Arrows indicate dilated cisternae of type five cells uniting with their cell membranes.

ER: endoplasmic reticulum

DL: distal layer

N: nucleus

PL: proximal layer

T₅: type five cell

X 8,350



Figure 69

Low-power view of the loose fibrous layer and adjacent structures of a stage five larva. Arrows indicate fine cytoplasmic processes.

CD: collecting duct

DF: dense fibrous layer

LF: loose fibrous layer

T₅: type five cell X 4,260

Figure 70

High-power view of a cross section of a terminal organ of a proto-nephridial system of a stage five larva.

F: flame

FC: flame cell

FR: flame cell rod

LF: loose fibrous layer

NC: nephridial funnel cell

NR: nephridial funnel cell rod

T₅: type five cell X 16,970

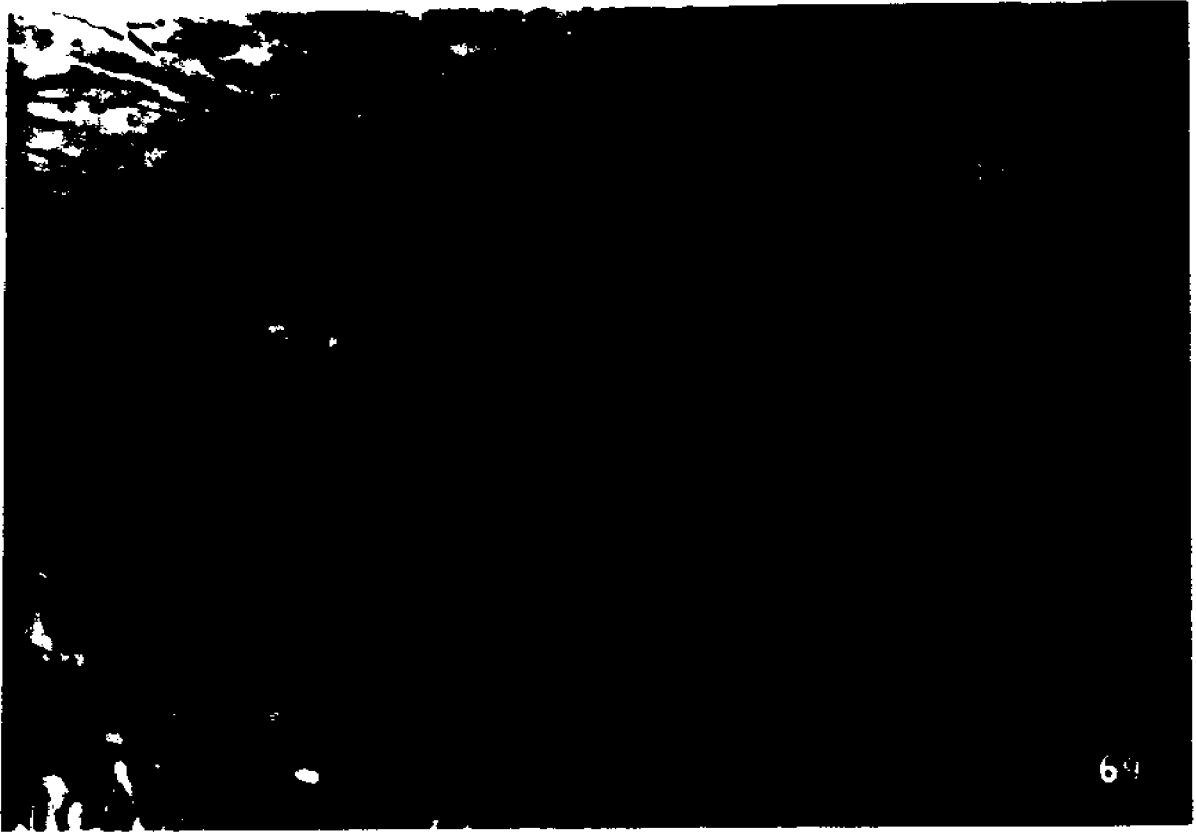


Figure 71

High-power view of a cross section through the interdigitated region of the terminal organ of a stage five larva.

F: flame

FC: flame cell

FR: flame cell rod

LF: loose fibrous layer

NC: nephridial funnel cell

NR: nephridial funnel cell rod X 16,970

Figure 72

High-power view of a cross section through the tip of the flame of a stage five larva. Arrows indicate fine cytoplasmic processes interspersed in the loose fibrous layer.

F: flame

LF: loose fibrous layer

NC: nephridial cell X 16,970



Figure 73

Low-power view of the dense fibrous layer of a stage five larva with type six cells and their cytoplasmic processes.

DF: dense fibrous layer

LD: lipid droplet

LF: loose fibrous layer

T₆: type six cell X 4,260

Figure 74

High-power view of a cross section of collecting ducts of a stage five larva. Arrows indicate bead-like cytoplasmic processes.

CD: collecting duct

LD: lipid droplet

LF: loose fibrous layer

T₆: type six cell X 16,970



Figure 75

The loose fibrous layer, the dense fibrous layer, and the invaginated scolex of a stage five larva.

DF: dense fibrous layer

IS: invaginated scolex

LF: loose fibrous layer

MT: microtrich

P: parenchymal cell

T: tegument

X 9,000



Figure 76

High-power view of the dense fibrous layer of a stage five larva.
Arrows indicate clusters of beta glycogen granules.

DF: dense fibrous layer

IS: invaginated scolex

LF: loose fibrous layer

MT: microtrich

N: nucleus

NS: nucleolus

P: parenchymal cell

T: tegument

T₆: type six cell

X 15,600

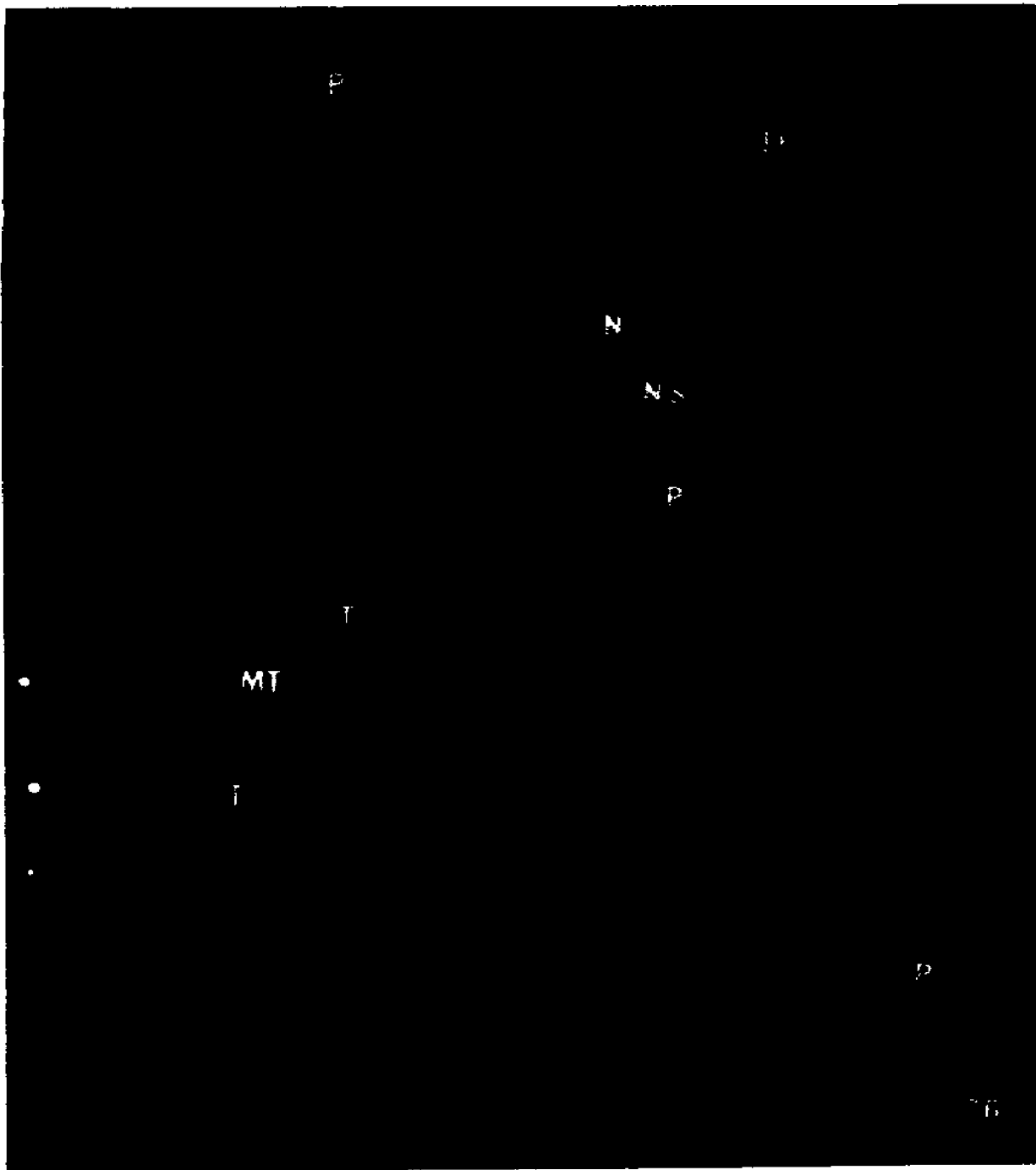


Figure 77

Low-power view of the dense fibrous layer of a stage five larva with several calcareous corpuscles.

CC: calcareous corpuscle

CD: collecting duct

X 5,140

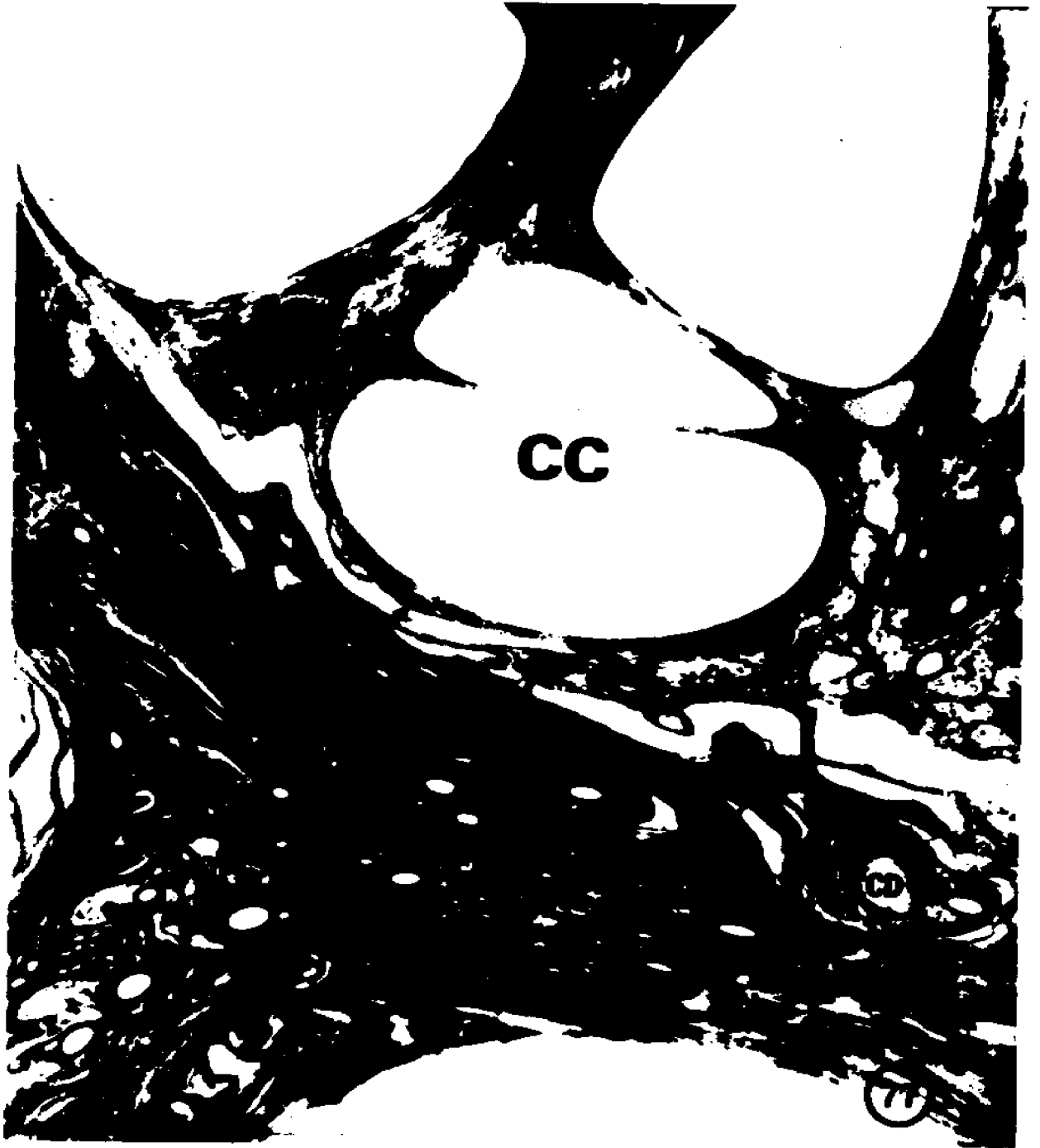


Figure 78

An atrophing calcareous corpuscle formation cell of a stage five larva.

CC: calcareous corpuscle

N: nucleus

X 9,000

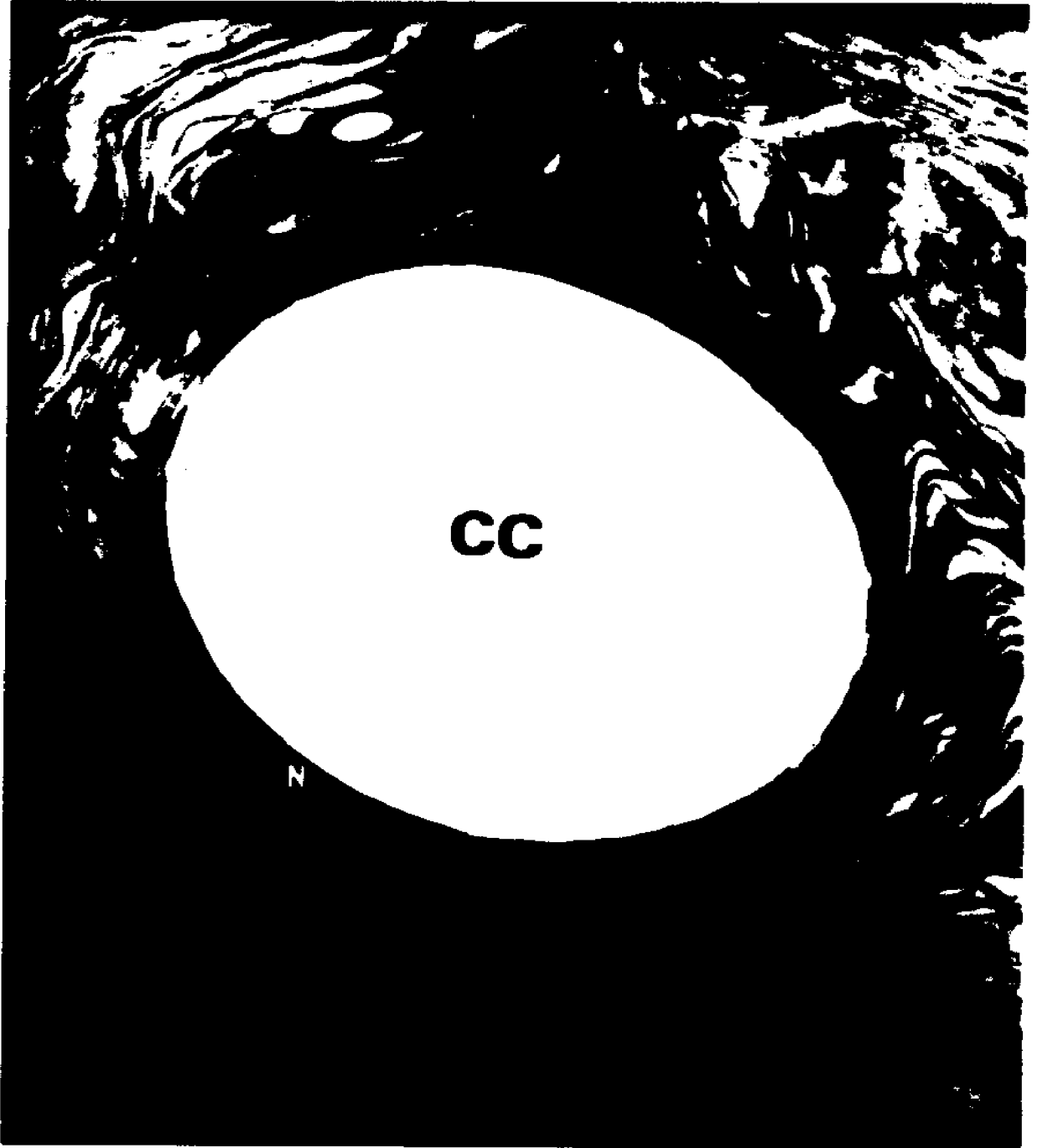


Figure 79

The tegument of an invaginated scolex and the dense fibrous layer of a stage five larva.

DF: dense fibrous layer

IS: invaginated scolex

MS: muscle

MT: microtrich

T: tegument

X 15,600



Figure 80

Low-power view of the sucker region of the invaginated scolex of a stage five larva.

DF: dense fibrous layer

MS: muscle

T: tegument

X 4,900

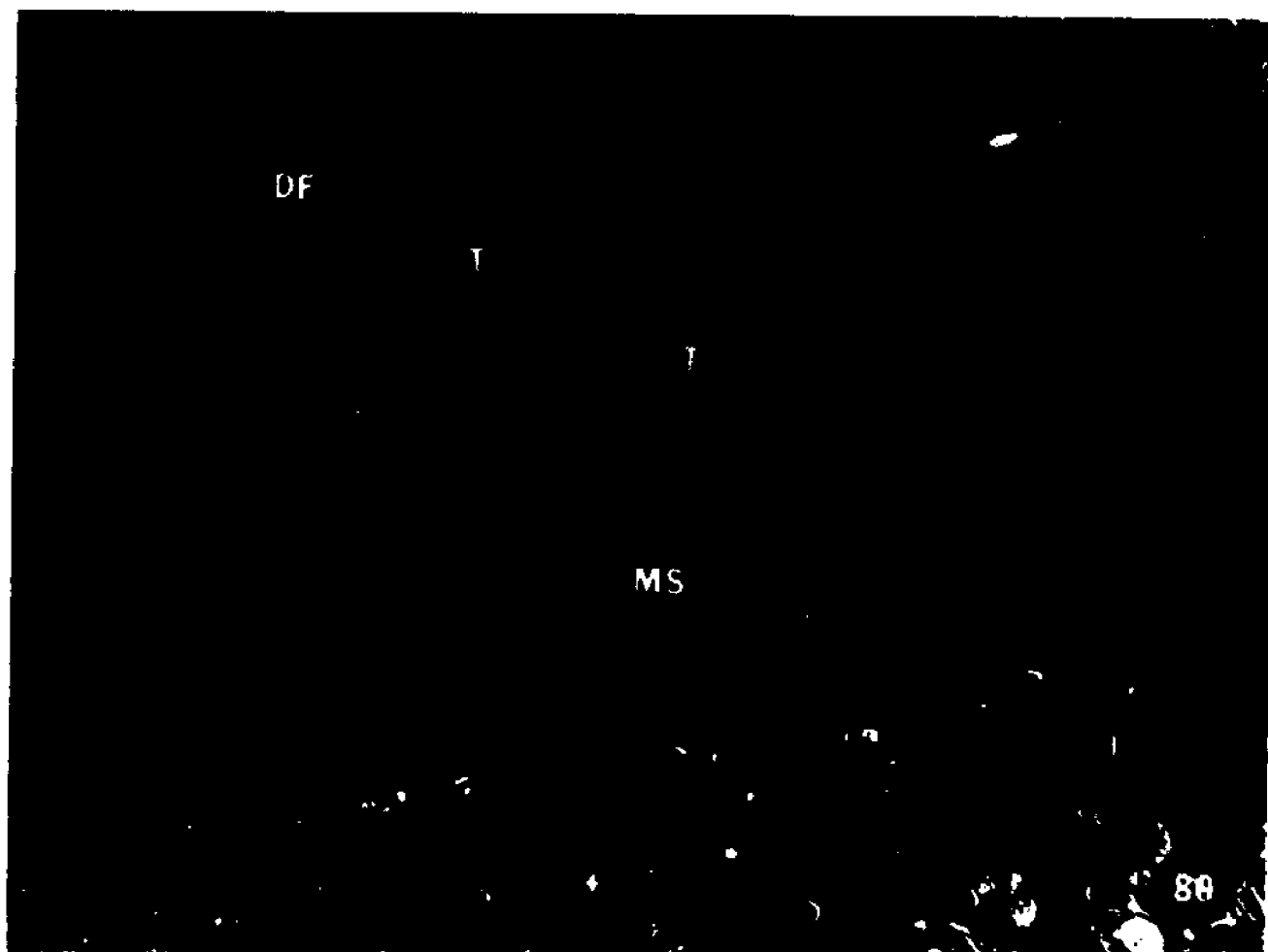


Figure 81

Low-power view of the inter-sucker region of the invaginated scolex of a stage five larva.

DF: dense fibrous layer

IS: invaginated scolex

MS: muscle

T: tegument

X 5,140



Figure 82

High-power view of the anterior canal of a stage five larva.

AC: anterior canal

T: tegument

V: microvilli

X 20,880



Figure 83

Low-power view of the plug and the dense fibrous layer of a stage five larva.

CD: collecting duct

DF: dense fibrous layer

P: parenchymal cell

PG: plug

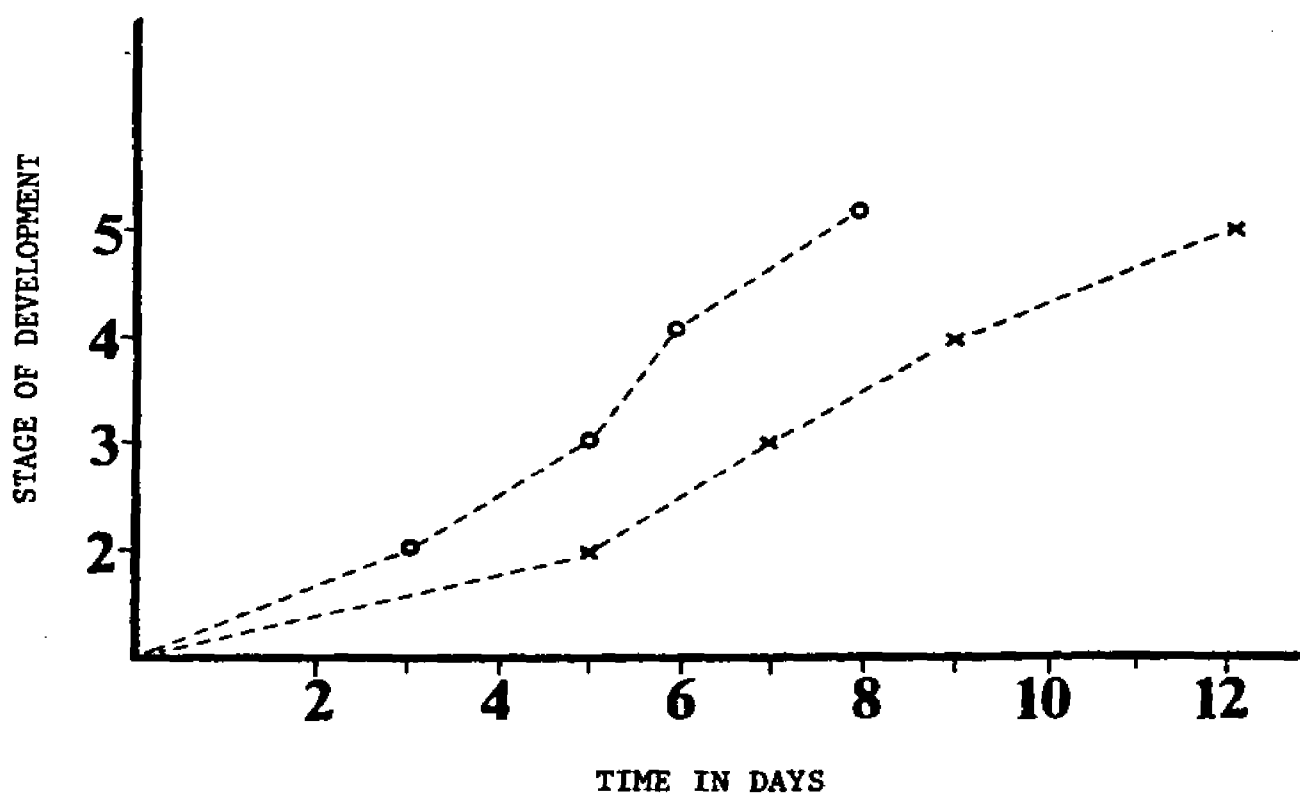
T₆: type six cell

VC: vesicle

X 5,140



A growth curve of the postembryonic development of Hymenolepis diminuta in the intermediate hosts.



- o -- The confused flour beetles, *Tribolium confusum* served as an intermediate host and were maintained at 30°C
- x -- The grain beetles, *Tenebrio molitor* served as an intermediate host and were maintained at 25°C

Figure 84

APPENDIX II

PREPARATION OF A POLYCHROME STAIN

A polychrome stain for Epoxy-Embedded Tissue (Sato and Shamato, 1973)

The staining solution was prepared as follows:

Monobasic sodium phosphate	0.5 gm.
Basic fuchsin	0.25 gm.
Methylene blue	0.2 gm.
0.5% Boric acid	15 ml.
Distilled water	70 ml.

Dissolve the above chemicals in distilled water. 10 ml.
of 0.72% Naoh was added in the above mixture.

Sections were stained for 20 to 30 seconds at 45°C to 50°C and dried after ringing. An immersion oil mounting sealed with epoxy resin prevents the stain from fading for at least one year.

LITERATURE CITED

- Allison, V. F., J. E. Ubelaker, and N. B. Cooper. 1972. The fine structure of the cysticeroid of Hymenolepis diminuta. II. The inner wall of the capsule. *Z. Parasitenk.* 39: 137-147.
- Baron, J. P. 1968. On the histology and ultrastructure of Cysticercus longicollis, the cysticercus of Taenia crassiceps Zeder, 1800 (Cestoda: Cyclophyllidea). *Parasitology* 59: 497-513.
- Baron, J. P. 1971. On the histology, histochemistry and ultrastructure of the cysticeroid of Raillietina cestocillus (Molin, 1858). Fuhrmann, 1920 (Cestoda: Cyclophyllidea). *Parasitology* 62: 233-235.
- Bonsdorff, C. H. von and A. Telkka. 1966. The flagellar structure of the flame cell in fish tapeworm (Diphyllobothrium latum). *Z. Zellforsch. mikrosk. Anat.* 70: 169-179.
- Brand, T. von, T. I. Mercado, M. U. Nylen, and D. B. Scott. 1960. Observations on function, composition, and structure of cestode calcareous corpuscles. *Exp. Parasit.* 9: 205-214.
- Braten, T. 1968a. An electron microscope study of the tegument and associated structures of the proceroid of Diphyllobothrium latum. *Z. Parasitenk.* 30: 104-112.
- Braten, T. 1968b. The fine structure of the tegument of Diphyllobothrium latum. A comparison of the plerocercoid and adult stages. *Z. Parasitenk.* 30: 104-112.
- Chowdhury, A. B., B. Dasgupta, and H. N. Ray. 1962. On the nature and the structure of the calcareous corpuscles in Taenia saginata. *Parasitology* 52: 153-157.
- Collin, W. K. 1968. Electron microscope studies of the muscle and hook systems of hatched oncospheres of Hymenolepis citelli. McLeod, 1933 (Cestode: Cyclophyllidea). *J. Parasit.* 54: 74-8.
- Collin, W. K. 1969. The cellular organization of hatched oncospheres of Hymenolepis citelli (Cestoda: Cyclophyllidea). *J. Parasit.* 55: 149-166.
- Collin, W. K. 1970. Electron microscopy of postembryonic stage of the tapeworm Hymenolepis citelli. *J. Parasit.* 56: 1159-1170.

- Cooper, N. B., V. F. Allison, and J. E. Ubelaker. 1975. The fine structure of the cysticeroid of Hymenolepis diminuta. Z. Parasitenk. 46: 229-239.
- Featherston, D. W. 1972. Taenia hydatigena. IV. Ultrastructure study of the tegument. Z. Parasitenk. 38: 214-232.
- Howells, R. E. 1965. Electron microscope and histochemical studies on the cuticle and subcuticular tissues of Monizia expansa. Parasitology. 55: 20-21.
- Howells, R. E. 1969. Observations on the nephridial system of the cestode Moniezia expansa. Parasitology. 59: 449-459.
- Jha, R. K. 1969. Echinococcus granulosus: Ultrastructure of microtriches. Exp. Parasit. 25: 232-244.
- Lethbridge, R. C. 1971. The hatching of Hymenolepis diminuta eggs and penetration of the hexachths in Tenebria molitor beetles. Parasitology. 62: 445-456.
- Lumsden, R. D., and J. Byram III. 1967. The ultrastructure of cestode muscle. J. Parasit. 53: 326-342.
- Martin, W. E. and R. F. Bills. 1964. Trematode excretory concretions: formation and fine structure. J. Parasit. 40: 337-344.
- Morseth, D. J. 1967. Fine structure of the hydatid cyst and protoscolex of Echinococcus granulosus. J. Parasit. 53: 312-325.
- Nieland, M. L. and T. von Brand. 1969. Electron Microscopy of cestode calcareous corpuscle formation. Exp. Parasit. 24: 279-289.
- Ogren, R. E. 1962. Continuity of morphology from oncosphere to early cysticeroid in the development of Hymenolepis diminuta (Cestoda: Cyclophyllidea). Exp. Parasit. 12: 1-6.
- Ogren, R. E. 1972. Basic hook musculature in invasive oncospheres of the tapeworm Hymenolepis diminuta. J. Parasit. 58: 240-243.
- Race, C. J., J. E. Larsh, G. W. Essh, and J. H. Martin. 1965. A study of the larval stages of Multiceps serialis by electron microscopy. J. Parasit. 51: 364-369.
- Reynolds, E. S. 1963. The use of lead citrate at high pH as an electron opaque stain in electron microscopy. J. Cell. Biol. 17: 208-212.

- Rifkin, E., T. C. Cheng, and H. R. Hohl. 1970. The fine structure of the tegument of Tylocephalum metacestodes: with emphasis on a new type of microvilli. *J. Morph.* 130: 11-24.
- Rothman, A. H. 1957. The larval development of Hymenolepis diminuta and H. citelli. *J. Parasit.* 43: 642-648.
- Rothman, A. H. 1963. Electron microscopic studies of tapeworms: the surface structures of Hymenolepis diminuta (Rud., 1819; Blanchard, 1891). *Trans. Amer. micr. Soc.* 82: 22-30.
- Rybicka, K. 1966. Embryogenesis in cestodes. *Adv. Parasit.* 4: 107-186.
- Rybicka, K. 1973. Ultrastructure of the embryonic syncytial epithelium in a cestode Hymenolepis diminuta. *Parasit.* 66: 9-18.
- Sato, T. and M. Shamato. 1973. A simple rapid polychrome stain for epoxy-embedded tissue. *Stain Technology.* 48: 223-227.
- Skaer, R. J. 1965. The origin and continuous replacement of epidermal cells in the planarian Polycelis nigra. *J. Embr. Exptl. Morph.* 13: 129-139.
- Spurr, A. R. 1969. A low-viscosity epoxy resin embedding medium for electron microscopy. *J. Ultrastruct. Res.* 26: 31-43.
- Ubelaker, J. E., N. B. Cooper, and V. F. Allison. 1970a. The fine structure of the cysticercoid of Hymenolepis diminuta. I. The outer wall of the capsule. *Z. Parasitenk.* 34: 258-270.
- Ubelaker, J. E., N. B. Cooper, and V. F. Allison. 1970b. Possible defensive mechanism of Hymenolepis diminuta cysticercoids to haemocytes of the beetle Tribolium confusum. *J. Invert. Path.* 16: 310-312.
- Voge M. and D. Heyneman. 1957. Development of Hymenolepis nana and Hymenolepis diminuta (Cestoda: Cyclophyllidea) in the intermediate host Tribolium confusum. *Univ. Calif. Publ. Zool.* 59: 549-580.
- Voge, M. 1960. Studies in cysticercoid histology. IV. Observations on histogenesis in the cysticercoid of Hymenolepis diminuta (Cestoda: Cyclophyllidea). *J. Parasit.* 46: 717-725.
- Voge, M. 1961. Studies on cysticercoid histology. V. Observations on the fully developed cysticercoid of Hymenolepis citelli (McLeod, 1933) (Cestoda: Cyclophyllidea). *Proc. Helm. Soc. Wash.* 28: 1-3.

- Watson, M. L. 1958. Staining of tissue sections for electron microscopy with heavy metals. *J. Viophys. Biochem. Cytol.* 4: 475-478.
- Wilson, R. A. 1969. The fine structure of the protonephridial system in the miracidium of Fasciola hepatica. *Parasitology.* 59: 461-467.
- Wilson, R. A. and L. A. Webster. 1974. Protonephridia. *Camb. Phyl. Soc. Biol. Rev.* 49: 127-160.